Quantum Completion of the Axis Model: Gauge Structure, BRST Invariance, and Renormalization Stability

Andrew Morton, MD

Adjunct Clinical Assistant Professor, Indiana University School of Medicine

Independent Researcher[*]

September 14, 2025

Abstract

This paper completes the quantum formalism of the Axis Model, a geometric unification framework in which all observable particles are constructed as scalar-stabilized tri-vector composites known as mortons. We derive the full operator content of the scalar, vector, and fermionic sectors; construct the gauge–covariant derivative from internal projection geometry; dynamically derive the electroweak $SU(2)_L \times U(1)_Y$ sector; and demonstrate BRST invariance, unitarity, and anomaly cancellation. The gauge fields arise as projections of Abelian vector modes onto internal symmetry generators, and scalar coherence enforces both gauge invariance and topological consistency. We show that the quantum theory is renormalizable and radiatively stable throughout the effective-field-theory window $E_{\mathrm{IR}} < \mu < \min(\Lambda_\Phi, \Lambda_q)$, with a scalar-coherence cutoff $\Lambda_\Phi \sim 10^5 \, \mathrm{GeV}$ and a morton-dissolution scale $\Lambda_q \sim 10^{16} \, \mathrm{GeV}$. Within this window, all low-energy predictions match the Standard Model, and in the infrared the theory reduces to a *constrained* SMEFT with sub-percent operator deviations. Taken together, these results establish the Axis Model as a quantum-consistent effective field theory across its validity window.

---

[*]This work was conducted independently and does not represent the views of Indiana University.

Introduction

The Axis Model is a geometric unification framework in which all matter and gauge structure emerges from the internal configuration of scalar-stabilized vector displacements, termed mortons. Prior work has shown that the Standard Model's full fermion spectrum and mixing matrices—and the electroweak gauge sector—can be derived from first principles within this structure [1]. However, to establish the Axis Model as a quantum-consistent effective field theory, one must demonstrate its consistency as a quantum field theory across its validity window.

This paper provides that quantum completion at the EFT level. We formulate the full operator structure of the scalar, vector, and fermionic sectors; construct gauge-invariant dynamics via projection-filtered covariant derivatives; and show that the resulting quantum action satisfies BRST invariance and unitarity. The gauge fields arise not as fundamental inputs but as emergent projections of internal vector displacements, filtered by scalar coherence and constrained by the internal symmetry algebra.

Anomaly cancellation is shown to be a geometric consequence of scalar-bundle triviality: only those fermion configurations that preserve the global coherence of the scalar phase survive. The scalar field thus serves as both a dynamical stabilizer and a topological anomaly detector.

We further demonstrate radiative stability under renormalization-group flow. One-loop beta functions for the geometric couplings are computed, and the scalar vacuum remains stable up to the scalar-coherence scale $\Lambda_\Phi \sim 10^5$ GeV. Toward the infrared, the model matches smoothly to the Standard Model Effective Field Theory and the chiral Lagrangian description of QCD.

For clarity, we interpret the construction as a predictive EFT on $E_{\text{IR}} < \mu < \min(\Lambda_\Phi, \Lambda_q)$, with Λ_Φ and Λ_q defined above and detailed in §4.1. Within this window the theory admits a BRST-invariant, unitary quantization, is renormalizable and radiatively stable, and matches the Standard Model in the IR (reducing to a constrained SMEFT).

1 Gauge Invariance from Morton Geometry

1.1 Local Symmetry Transformations on Morton States

The Axis Model postulates that all observable matter fields are scalar-stabilized tri-vector configurations known as mortons. Each morton is composed of quantized internal displacements along orthogonal geometric axes—typically the x-axis, associated with spatial and electromagnetic interactions, and the z-axis, associated with mass and gravitational structure. The internal arrangement of these vectors defines a localized internal configuration space at each spacetime point. When considered collectively across multiple mortons, these configurations naturally admit a local transformation structure corresponding to the gauge groups of the Standard Model.

Internal states as geometric fields. We formalize the internal projection geometry of mortons using quantum fields constructed from their constituent vector displacements.

Electroweak interactions: Each morton contains two x-axis displacements. The internal configuration of these vectors is represented as a two-component spinor field:

$$\chi(x) = \begin{pmatrix} v_x^{(1)}(x) \\ v_x^{(2)}(x) \end{pmatrix}, \qquad \chi(x) \in \mathbb{C}^2.$$

Under a local $SU(2)$ gauge transformation, this field transforms as:

$$\chi(x) \to U_2(x)\,\chi(x), \qquad U_2(x) \in SU(2).$$

Color interactions: The internal SU(3) color degree of freedom does not arise from an individual morton, but from a composite structure—specifically, a triplet of mortons such as those forming a baryon. Each of the three mortons contributes one z-axis displacement. The resulting internal configuration of the triplet is represented as:

$$\psi(x) = \begin{pmatrix} v_z^{(\text{quark 1})}(x) \\ v_z^{(\text{quark 2})}(x) \\ v_z^{(\text{quark 3})}(x) \end{pmatrix}, \qquad \psi(x) \in \mathbb{C}^3.$$

Under a local $SU(3)$ gauge transformation, this composite field transforms as:

$$\psi(x) \to U_3(x)\,\psi(x), \qquad U_3(x) \in SU(3).$$

This internal triplet structure reflects the emergent color degree of freedom in the Axis Model. It arises dynamically from the coherent alignment of z-axis displacements across bound morton composites, rather than from the structure of any individual morton. As shown in the Standard Model derivation paper [1], the $SU(3)$ symmetry is understood as emerging from the internal configuration geometry of these triplets, corresponding to the coset manifold:

$$CP^2 \cong \frac{SU(3)}{SU(2) \times U(1)}.$$

Necessity of a connection field. To maintain internal coherence under local transformations, the standard derivative $\partial_\mu \chi(x)$ or $\partial_\mu \psi(x)$ must be promoted to a gauge-covariant derivative. For example:

$$\partial_\mu \chi(x) \to U_2(x)\,\partial_\mu \chi(x) + (\partial_\mu U_2(x))\,\chi(x),$$

violates gauge invariance unless a connection field is introduced to absorb the inhomogeneous term. We therefore define:

$$D_\mu \chi(x) = \partial_\mu \chi(x) - ig A_\mu^a(x) T^a \chi(x),$$

where $A_\mu^a(x)$ is a connection field taking values in the Lie algebra of the internal symmetry group, and T^a are the corresponding generators.

The appearance of a gauge field is thus not imposed arbitrarily; it is a mathematical necessity for preserving the internal geometric symmetry under local transformations.

1.2 Construction of the Covariant Derivative

In the Axis Model, gauge fields are not fundamental but arise from geometric projections of internal vector displacements in the morton configuration space. Specifically, we construct the non-Abelian gauge fields $A_\mu^a(x)$ as **projections** of the underlying Abelian fields $X_\mu(x)$ and $Z_\mu(x)$, filtered through the symmetry structure of the local morton state.

Projection onto internal symmetry generators. Let T^a denote the generators of the relevant Lie algebra (e.g., the Pauli matrices for $SU(2)$, the Gell-Mann matrices for $SU(3)$). The morton configuration at spacetime point x is encoded in a projection matrix $\mathcal{V}(x)$, constructed from the internal displacement vectors $\vec{v}_i(x) \in \{\vec{v}_x, \vec{v}_z\}$. A natural choice is:

$$\mathcal{V}(x) = \sum_{i=1}^{N} \vec{v}_i(x) \otimes \vec{v}_i^\dagger(x),$$

which encodes the local geometric structure of the morton state $q(x)$.

We define a geometric projection operator P^a that selects the component of the combined field content $\{X_\mu, Z_\mu\}$ aligned with generator T^a as:

$$A_\mu^a(x) = P^a \left[X_\mu(x), Z_\mu(x), q(x)\right] \equiv \text{Tr}\left[T^a \cdot \mathcal{V}_\mu(x)\right], \tag{1}$$

where $\mathcal{V}_\mu(x)$ is a linear combination of internal projection displacements modulated by X_μ, Z_μ, and scalar coherence factors. The specific form of $\mathcal{V}_\mu(x)$ depends on the axis-aligned content of the morton and the scalar field background $\Phi(x)$, but its key role is to **project the Abelian vector content onto the symmetry algebra of the internal space**.

Constructing the covariant derivative. With this emergent gauge field $A_\mu^a(x)$, we define the covariant derivative acting on internal morton fields as:

$$D_\mu = \partial_\mu - ig A_\mu^a(x) T^a = \partial_\mu - ig \left(P^a \left[X_\mu, Z_\mu, q(x)\right]\right) T^a. \tag{2}$$

This operator ensures local gauge covariance under internal transformations $q(x) \to U(x)q(x)$, where $U(x) \in G$, by construction: the projection depends explicitly on the internal structure of the state $q(x)$, so its variation under transformation ensures proper compensation of $\partial_\mu \to D_\mu$.

Non-Abelian structure from commutators. The field strength tensor arises from the commutator of covariant derivatives:

$$[D_\mu, D_\nu] = -ig F_{\mu\nu}^a(x) T^a,$$

where:

$$F_{\mu\nu}^a = \partial_\mu A_\nu^a - \partial_\nu A_\mu^a + g f^{abc} A_\mu^b A_\nu^c,$$

and f^{abc} are the structure constants of the Lie algebra.

In this construction, the nonlinear term $f^{abc} A_\mu^b A_\nu^c$ is not imposed—it arises **naturally** from the fact that the projection operators P^a act on a non-commutative basis $\{T^a\}$. The internal geometry of the morton state induces curvature in the projection space, and the scalar field coherence ensures that the non-Abelian structure is preserved under evolution.

Conclusion. The covariant derivative in the Axis Model is not postulated but is instead derived from projection geometry. Gauge invariance emerges as a necessary condition to maintain local symmetry across the internal projection space. The vector fields A_μ^a are filtered combinations of fundamental Abelian fields X_μ, Z_μ, and their structure reflects the symmetries of the composite morton configuration. This construction geometrically enforces the Standard Model gauge structure from first principles.

1.3   From Projection Geometry to a Consistent Quantum Theory

The preceding construction shows that gauge invariance in the Axis Model arises directly from projection geometry and is therefore structurally unavoidable. Because a reader might interpret the projection step as an ad hoc assumption, it is useful to make explicit why this mechanism is the necessary link that connects local symmetry on morton states to a consistent quantum field theory. The logical chain is:

$$\text{projection} \;\Rightarrow\; \text{connection} \;\Rightarrow\; \text{curvature} \;\Rightarrow\; \text{BRST-invariant quantum theory},$$

as developed in Sections 1–3 of this work.

1) Projection as a necessary connection.   Morton internal degrees of freedom transform under local $SU(2)$ and $SU(3)$ actions. Under $U(x) \in G$, the inhomogeneous term $(\partial_\mu U)\chi$ in $\partial_\mu \chi(x)$ requires a compensating connection $A_\mu^a T^a$. In the Axis Model this connection is derived as a projection of (X_μ, Z_μ) through the local morton geometry $V(x)$:

$$A_\mu^a(x) \;=\; P^a[X_\mu(x), Z_\mu(x), q(x)] \;\equiv\; \mathrm{Tr}\big[T^a \cdot V_\mu(x)\big], \tag{3}$$

with covariant derivative

$$D_\mu = \partial_\mu - ig\, A_\mu^a T^a. \tag{4}$$

Thus the gauge fields are not optional insertions but the minimal geometric structure required to preserve local symmetry in morton projection space.

2) BRST invariance from the projected connection.   Once the connection is fixed by projection, the standard BRST completion follows, as detailed in Section 2.2. Gauge fixing in R_ξ introduces ghosts $c^a, \bar{c}^a$, and the nilpotent BRST transformations are

$$sA_\mu^a = D_\mu^{ab} c^b, \qquad\qquad s\psi = ig\, c^a T^a \psi, \tag{5}$$

$$sc^a = -\tfrac{1}{2} f^{abc} c^b c^c, \qquad\qquad s\bar{c}^a = \xi^{-1} \partial^\mu A_\mu^a, \quad s\Phi = 0, \tag{6}$$

with $s^2 = 0$ and

$$s(L_{\mathrm{Axis}} + L_{\mathrm{GF}} + L_{\mathrm{ghost}}) = 0.$$

The projected gauge field therefore supports a complete BRST-invariant quantization, with the physical Hilbert space defined by the cohomology of Q_{BRST}.

3) Anomaly cancellation via scalar bundle triviality.   Anomaly cancellation in this framework is not imposed by hand, but is enforced by the topological constraints of the scalar field, as shown in Section 3. The scalar bundle condition $c_1(\Phi) = 0$ enforces global triviality of the scalar coherence phase. Any fermion configuration producing a nonvanishing anomaly trace would destabilize morton formation and is therefore dynamically excluded. This mechanism reproduces the Standard Model's anomaly-free structure as a geometric selection rule.

4) Anchor in the master Lagrangian.   All of these elements are encoded in the master Lagrangian,

$$\begin{aligned}
\mathcal{L}_{\mathrm{Axis}} = &\tfrac{1}{2}(\partial\Phi)^2 - V(\Phi) - \tfrac{1}{4}F_X^2 + \tfrac{1}{2}g_{X\Phi}^2 \Phi^2 X_\mu X^\mu - \tfrac{1}{4}F_Z^2 + \tfrac{1}{2}g_{Z\Phi}^2 \Phi^2 Z_\mu Z^\mu \\
&+ \bar{\psi}\,(i\,\slashed{\partial} - m_\psi - g_{\psi\Phi}\Phi)\psi + g_{\psi Z}\,\bar{\psi}\gamma^\mu Z_\mu \psi \\
&+ \frac{g_A}{M}\,\Phi_A F_X \tilde{F}_X + g_Z(\partial_\mu \Phi) Z^\mu,
\end{aligned} \tag{7}$$

which underlies the quantization, BRST analysis, and loop-level corrections.

Here the explicit fermion–vector coupling

$$g_{\psi Z}\,\bar{\psi}\gamma^{\mu}Z_{\mu}\psi$$

is included. This term is essential for the BRST transformation of the fermion field,

$$s\psi \;=\; -ig_Z\,c_Z\,\psi,$$

ensuring that the fermion sector transforms consistently with the gauge–ghost sector. Its presence makes the link between the geometric Lagrangian and the BRST analysis explicit and complete.

Conclusion. Projection is the unique geometric realization of the connection required by local symmetry. Once established, it supports BRST invariance, anomaly cancellation, and unitarity. Far from being ad hoc, the projection mechanism is the structural necessity that makes the Axis Model a consistent quantum field theory.

2 Quantum Completion: Operator Formalism and Hilbert Space

To elevate the Axis Model from a classical geometric framework to a quantum field-theoretic structure, we formalize the operator content of the scalar, vector, and fermionic sectors, define their Hilbert space, and demonstrate gauge consistency via BRST quantization. This section shows that the model satisfies unitarity, ghost cancellation, and gauge invariance at the level of the quantum effective action.

2.1 Quantized Morton States and Internal Hilbert Space

Mortons are defined as tri-vector composites stabilized by scalar coherence. To quantize them, we interpret each internal displacement vector $\vec{v}_i \in \{\vec{v}_x, \vec{v}_z\}$ as a basis state in an internal Fock space. The full morton state becomes a composite of three excitations:

$$|q\rangle = a_i^{\dagger}a_j^{\dagger}a_k^{\dagger}|0\rangle, \tag{8}$$

where $a^{\dagger}$ are creation operators for quantized internal displacements. As these represent geometric excitations, they are assumed to obey standard bosonic commutation relations:

$$[a_i, a_j^{\dagger}] = \delta_{ij}.$$

The scalar field $\Phi(x)$ mediates binding coherence and entanglement, and thus defines an effective wavefunction over internal projection space:

$$|\Psi_{\mathrm{morton}}(x)\rangle = \Phi(x)\,|v_1\rangle \otimes |v_2\rangle \otimes |v_3\rangle.$$

This forms a fiber bundle structure over spacetime with internal Hilbert fibers parameterized by scalar phase alignment.

Operator content. The fields quantized in this sector include the scalar coherence field $\Phi(x)$, which is real and dynamical; the Abelian vector fields $X_{\mu}(x)$ and $Z_{\mu}(x)$, which originate from internal x-axis and z-axis displacement structures, respectively; and the composite fermionic field $\psi_q(x)$, which represents a morton-bound state formed from coherent internal excitations.

These fields obey canonical equal-time commutation or anticommutation relations, depending on spin-statistics.

2.2 BRST Quantization and Gauge-Fixed Action

Gauge invariance in the Axis Model emerges from geometric projection symmetry, but to define a consistent quantum theory, we must show that this symmetry survives gauge fixing, and that no unphysical degrees of freedom (ghosts) violate unitarity. This is accomplished via BRST quantization, with the full BRST construction given here in Secs. 2.2–2.3; Appendix X of [2] now provides a concise summary

Gauge-fixing structure. We add to the Lagrangian a gauge-fixing term in covariant R_ξ gauge:

$$\mathcal{L}_{\text{GF}} = -\frac{1}{2\xi} \left(\partial^\mu A_\mu^a\right)^2,$$

which breaks manifest gauge invariance but introduces compensating ghost fields.

Ghost sector. We introduce anticommuting ghost and anti-ghost fields $c^a, \bar{c}^a$, and define the ghost Lagrangian:

$$\mathcal{L}_{\text{ghost}} = \bar{c}^a \, \partial^\mu D_\mu^{ab} c^b,$$

where $D_\mu^{ab} = \delta^{ab}\partial_\mu + gf^{abc}A_\mu^c$ is the covariant derivative in the adjoint representation. These fields cancel unphysical gauge modes in the loop expansion.

BRST transformations. We define a nilpotent BRST operator s, acting on the fields as:

$$sA_\mu^a = D_\mu^{ab} c^b, \tag{9}$$

$$s\psi = igc^a T^a \psi, \tag{10}$$

$$sc^a = -\frac{1}{2}gf^{abc}c^b c^c, \tag{11}$$

$$s\bar{c}^a = \frac{1}{\xi}\partial^\mu A_\mu^a, \tag{12}$$

$$s\Phi = 0. \tag{13}$$

One confirms that $s^2 = 0$, and the total action is BRST-invariant:

$$s(\mathcal{L}_{\text{Axis}} + \mathcal{L}_{\text{GF}} + \mathcal{L}_{\text{ghost}}) = 0.$$

Path integral formulation. The full quantum theory is defined via the BRST-invariant generating functional:

$$\mathcal{Z} = \int \mathcal{D}\Phi \, \mathcal{D}A \, \mathcal{D}c \, \mathcal{D}\bar{c} \, \mathcal{D}\psi \, \exp\left(i \int d^4x \, \mathcal{L}_{\text{eff}}\right),$$

where $\mathcal{L}_{\text{eff}} = \mathcal{L}_{\text{Axis}} + \mathcal{L}_{\text{GF}} + \mathcal{L}_{\text{ghost}}$.

Loop-level diagrams and beta functions are analyzed in Secs. 4.2–4.4 of this paper; Appendix X of [2] summarizes the results.

2.3 Physical State Condition and Unitarity

The consistency of the quantum theory is guaranteed by the physical state condition. We define a conserved, nilpotent BRST charge operator Q_{BRST}, which generates the BRST symmetry on operator-valued fields. The physical Hilbert space is then defined as the kernel of this operator:

$$Q_{\mathrm{BRST}}|\psi\rangle_{\mathrm{phys}} = 0. \tag{14}$$

This constraint ensures that all physical states are gauge-invariant and that all unphysical modes, including longitudinal polarizations, scalar gauge artifacts, and ghost excitations, decouple from any observable matrix element. The unitarity of the theory is thus preserved at all orders in perturbation theory.

Conclusion. We have shown that the Axis Model admits a fully consistent quantum field-theoretic formulation. All fields are quantized within a BRST-invariant path integral. Gauge fixing, ghost cancellation, and scalar coherence are incorporated in a unified framework, and physical state conditions guarantee unitarity. This completes the model's transition from a classical geometric theory to a renormalizable, unitary, and gauge-consistent quantum field theory.

3 Anomaly Cancellation via Scalar Topology

The Standard Model is known to be free of all gauge and gravitational anomalies, but this cancellation is typically imposed algebraically through a delicate balancing of fermion representations. In the Axis Model, anomaly cancellation is not inserted—it emerges as a consequence of scalar bundle coherence. In this section, we show that the vanishing of the first Chern class of the scalar field bundle implies the cancellation of all triangle anomalies in the effective theory, including the chiral $U(1)_Y^3$, mixed gauge-gravitational, and mixed $SU(2)^2 \times U(1)$ anomalies.

3.1 Anomaly Triangle Structure and Scalar Phase Neutrality

Triangle anomalies in chiral gauge theories arise from diagrams involving three gauge current insertions at a fermion loop. The generic divergence of the axial current takes the form:

$$\partial_\mu J_5^\mu = \frac{1}{16\pi^2}\epsilon^{\mu\nu\rho\sigma}\,\mathrm{Tr}\,[F_{\mu\nu}F_{\rho\sigma}] = \frac{1}{16\pi^2}F_{\mu\nu}\tilde{F}^{\mu\nu}, \tag{15}$$

where $\tilde{F}^{\mu\nu} = \frac{1}{2}\epsilon^{\mu\nu\rho\sigma}F_{\rho\sigma}$ is the dual field strength.

In the Axis Model, each morton is defined on a coherent scalar background $\Phi(x) = e^{i\theta(x)}$, which defines a $U(1)$ principal bundle over internal configuration space. For the scalar field to consistently bind a morton, this bundle must be globally trivial: its first Chern class must vanish. That is, for any closed 2-cycle $\Sigma \subset \mathcal{M}_{\mathrm{internal}}$,

$$c_1(\Phi) = \frac{1}{2\pi}\int_\Sigma F = 0. \tag{16}$$

This requirement implies that the scalar field cannot support a net topological phase winding across internal configuration space. In turn, this constrains the allowed gauge current configurations such that their combined anomaly contribution integrates to zero over the scalar background. Therefore, the only fermionic configurations that remain stable are those for which the net anomaly trace cancels.

Implication for fermion triangle diagrams. Each triangle anomaly diagram corresponds to a winding in the scalar phase bundle. The gauge-variant part of the path integral measure transforms under a local gauge transformation $\delta\theta(x)$ as:

$$\delta\mathcal{L} \sim \delta\theta(x) \cdot \frac{1}{16\pi^2} F_{\mu\nu}\tilde{F}^{\mu\nu}. \tag{17}$$

This violates scalar phase coherence unless the prefactor vanishes globally. Thus, only fermionic configurations with vanishing anomaly coefficients are permitted, not by hand, but because scalar winding would otherwise destabilize morton formation.

Example: Cancellation of the $[SU(2)]^2 \times U(1)$ anomaly. In the Standard Model, the sum of hypercharges over all left-handed $SU(2)$ doublets must vanish:

$$\sum_{\text{doublets}} Y = 0.$$

In the Axis Model, this condition follows from the requirement that scalar coherence be preserved over the internal fiber bundle defined by left-handed morton configurations. The internal symmetry content of each morton configuration induces a local scalar curvature; if the total curvature summed over all families is non-zero, the associated gauge winding violates the condition in Eq. (16), and the configuration is projected out by scalar destabilization.

3.2 Chern–Simons Formalism and Cohomological Structure

To formalize this, we reinterpret the scalar field as defining a connection over a principal $U(1)$ bundle, and use standard cohomological tools to relate anomaly structure to topological class integrals. The anomaly density is given by the exterior derivative of the Chern–Simons 3-form:

$$d\omega_3 = \text{Tr}\left[F \wedge F\right], \tag{18}$$

where the Chern–Simons form is:

$$\omega_3 = \text{Tr}\left(A \wedge dA + \frac{2}{3} A \wedge A \wedge A\right).$$

The integral of this density over a closed 4-manifold is proportional to the instanton number, which in the presence of a nontrivial scalar field coupling would generate a gauge-violating term. Scalar coherence thus acts as a topological filter: it projects out any gauge configurations whose instanton number is nonzero, as these configurations would break the scalar's global triviality.

Topological triviality as anomaly filter. The scalar bundle's requirement $c_1(\Phi) = 0$ serves as a cohomological constraint that enforces anomaly cancellation at the global level. It corresponds to requiring that all fermionic triangle traces vanish in aggregate:

$$\text{Tr}[Y^3] = \text{Tr}[Y] = \text{Tr}[T^a\{T^b, Y\}] = 0,$$

for hypercharge Y and gauge generators T^a. Any failure of these conditions would be topologically visible in the scalar background and therefore dynamically suppressed.

3.3 From Scalar Coherence to Anomaly Cancellation: Determinant-Line Argument

Setup. Let Σ denote the Axis-Model internal configuration space supporting the emergent $SU(2)$ structure for fermionic morton composites (cf. App. A). Let $L_Y \to \Sigma$ be the hypercharge line bundle and $E_2 \to \Sigma$, $E_3 \to \Sigma$ the rank-2 and rank-3 bundles associated with the internal $SU(2)_L$ and $SU(3)_c$ fibers (cf. Master Lagrangian and fermion sector, App. M). A left-handed 4D Weyl fermion of representation (R_3, R_2, Y_f) is realized as a zero mode of an internal Dirac operator twisted by

$$\mathcal{E}_f \equiv (E_3)^{\otimes R_3} \otimes (E_2)^{\otimes R_2} \otimes L_Y^{\otimes Y_f}. \tag{19}$$

Let $\mathcal{D}_f$ be the corresponding 4D chiral Dirac operator on M_4, parametrized by background gauge fields (A_Y, W, G). The phase of the fermionic path-integral measure is a section of the *determinant line bundle* $\det \mathcal{D} \to \mathcal{A}/\mathcal{G}$ over the space of gauge fields modulo gauge equivalence; its curvature is the 6-form anomaly polynomial I_6 (Fujikawa/Bismut–Freed descent).

We adopt the conventions

$$T_2(\mathbf{2}) = \tfrac{1}{2}, \quad T_3(\mathbf{3}) = \tfrac{1}{2}, \qquad d_2(\mathbf{2}) = 2, \quad d_3(\mathbf{3}) = d_3(\overline{\mathbf{3}}) = 3,$$

and define the anomaly sums

$$S_1 \equiv \sum_f d_2(R_f)\, d_3(R_f)\, Y_f, \qquad\qquad S_3 \equiv \sum_f d_2(R_f)\, d_3(R_f)\, Y_f^3, \tag{20}$$

$$S_{2L} \equiv \sum_f Y_f\, T_2(R_f), \qquad\qquad S_{2C} \equiv \sum_f Y_f\, T_3(R_f). \tag{21}$$

With standard 4D normalizations, the anomaly polynomial is

$$I_6 = \frac{1}{24\pi^2}\Big[S_3\, F_Y^3 + 3\, S_{2L}\, F_Y \wedge \mathrm{tr}\big(F_2 \wedge F_2\big) \\ + 3\, S_{2C}\, F_Y \wedge \mathrm{tr}\big(F_3 \wedge F_3\big)\Big] + \frac{1}{192\pi^2}\, S_1\, F_Y \wedge \mathrm{tr}\big(R \wedge R\big). \tag{22}$$

where F_Y, F_2, F_3 are the $U(1)_Y$, $SU(2)$, $SU(3)$ curvatures and R is the spacetime Riemann curvature two-form.

Axis-Model coherence principle. *Global scalar-phase coherence* requires that the *combined family bundle*

$$\mathcal{E}_{\mathrm{fam}} \equiv \bigoplus_f \mathcal{E}_f \tag{23}$$

admits a coherent scalar trivialization on Σ which remains compatible with *all* admissible external gauge backgrounds. Equivalently, the induced determinant line over $\mathcal{A}/\mathcal{G}$ is *trivial (flat)*. In the anomaly language, this entails

$$I_6 \equiv 0 \quad \text{as a polynomial in } F_Y,\ F_2,\ F_3,\ R, \tag{24}$$

for arbitrary backgrounds.

Proposition (Coherence $\Rightarrow$ anomaly cancellation). If the scalar coherence principle holds, then

$$S_1 = 0, \qquad S_3 = 0, \qquad S_{2L} = 0, \qquad S_{2C} = 0, \tag{25}$$

i.e. the mixed gauge–gravity $U(1)_Y$, cubic $U(1)_Y^3$, and mixed $SU(2)^2 - U(1)_Y$, $SU(3)^2 - U(1)_Y$ anomalies vanish. Moreover, $SU(2)^3$ vanishes locally (pseudoreal doublet), $SU(3)^3$ vanishes for the SM family content (Sec. 3.5), and the Witten global $SU(2)$ anomaly is absent (even number of doublets).

Proof. The field-strength 2-forms F_Y, F_2, F_3 and the Riemann curvature 2-form R can be chosen independently (as differential 2-forms on M_4 or, formally, as independent variables). Since eq. (22) must vanish for *any* such choice, the coefficients S_1, S_3, S_{2L}, S_{2C} multiplying the independent 6-form monomials F_Y^3, $F_Y \wedge \mathrm{tr}(F_2 \wedge F_2)$, $F_Y \wedge \mathrm{tr}(F_3 \wedge F_3)$, and $F_Y \wedge \mathrm{tr}(R \wedge R)$ must vanish separately. This yields eq. (25). □

Bundle-level origin of $S_1 = 0$. Because the $SU(n)$ bundles have $c_1(E_2) = c_1(E_3) = 0$, the determinant of the family bundle obeys

$$c_1(\det \mathcal{E}_{\mathrm{fam}}) \;=\; \sum_f d_2(R_f)\, d_3(R_f)\, Y_f\, c_1(L_Y) \;=\; S_1\, c_1(L_Y)\,. \tag{26}$$

Scalar coherence requires $\det \mathcal{E}_{\mathrm{fam}}$ to be topologically trivial on Σ; unless $c_1(L_Y)$ itself vanishes (which would trivialize hypercharge), this enforces $S_1 = 0$.

Descent origin of $S_3, S_{2L}, S_{2C} = 0$. For a line bundle, $\mathrm{ch}\!\left(L_Y^{\otimes Y_f}\right) = \exp\!\left(Y_f\, c_1(L_Y)\right) = 1 + Y_f\, c_1 + \frac{1}{2}Y_f^2 c_1^2 + \frac{1}{6}Y_f^3 c_1^3 + \cdots$. The $U(1)_Y^3$ term in the index density picks out $\sum_f Y_f^3$ as the coefficient of $c_1(L_Y)^3$, yielding S_3 in (22). Similarly, the mixed terms arise from

$$\mathrm{ch}\!\left(E_2^{\otimes R_2}\right) = \mathrm{rk}(R_2) \;-\; \frac{T_2(R_2)}{8\pi^2}\, \mathrm{tr}\!\left(F_2 \wedge F_2\right) + \cdots, \quad \mathrm{ch}\!\left(E_3^{\otimes R_3}\right) = \mathrm{rk}(R_3) \;-\; \frac{T_3(R_3)}{8\pi^2}\, \mathrm{tr}\!\left(F_3 \wedge F_3\right) + \cdots, \tag{27}$$

so the cross-terms proportional to $c_1(L_Y) \wedge \mathrm{tr}(F_{2,3} \wedge F_{2,3})$ carry coefficients $\sum_f Y_f T_{2,3}(R_f)$, giving S_{2L} and S_{2C}. Flatness of $\det \mathcal{D}$ for arbitrary (F_Y, F_2, F_3) forces these to vanish. □

3.4 "Show, Don't Tell": Two Short Constructions

(a) Mixed gauge–gravity anomaly via winding ($S_1 = 0$). Let $\gamma \subset \Sigma$ be a nontrivial closed loop and perform a large $U(1)_Y$ gauge transformation with parameter α such that $\oint_\gamma \frac{d\alpha}{2\pi} = 1$. Each LH Weyl fermion contributes a Jacobian phase $e^{iY_f\alpha}$, with degeneracy $d_2(R_f)d_3(R_f)$ from its non-Abelian representation. Scalar coherence demands the total phase be unity for *every* loop and background:

$$\prod_f \exp\!\left(i\, d_2(R_f)d_3(R_f)\, Y_f \oint_\gamma d\alpha\right) \;=\; \exp\!\left(i2\pi S_1\right) \stackrel{!}{=} 1\,. \tag{28}$$

Because this must hold uniformly (including backgrounds with fractionalized holonomy inherited from $\mathcal{A}/\mathcal{G}$), coherence for all loops implies $\boxed{S_1 = 0}$. □

(b) Descent for $U(1)^3$, $SU(2)^2U(1)$, $SU(3)^2U(1)$. Under a $U(1)_Y$ gauge variation with parameter $\alpha(x)$, Fujikawa's method gives

$$\delta_\alpha \Gamma = \frac{1}{24\pi^2} \int_{M_4} \alpha(x) \Big[\underbrace{\textstyle\sum_f Y_f^3}_{S_3}\, F_Y \wedge F_Y + 3 \underbrace{\textstyle\sum_f Y_f T_2(R_f)}_{S_{2L}}\, \mathrm{tr}\!\left(F_2 \wedge F_2\right)$$

$$+ 3 \underbrace{\textstyle\sum_f Y_f T_3(R_f)}_{S_{2C}}\, \mathrm{tr}\!\left(F_3 \wedge F_3\right) \Big]\,. \tag{29}$$

11

In the Axis Model the $U(1)_Y$ parameter is the physical scalar phase along the internal y-axis; global scalar coherence requires $\delta_\alpha \Gamma \equiv 0$ for arbitrary admissible backgrounds, hence $S_3 = S_{2L} = S_{2C} = 0$. $\square$

3.5 Expanded Checks: $SU(3)^3$ and Witten $SU(2)$

$SU(3)^3$**.** Count (per generation) chiral color triplets in the LH basis. With $A(\mathbf{3})$ the cubic index for the fundamental (we take $A(\mathbf{3}) = \frac{1}{2}$ and $A(\bar{\mathbf{3}}) = -\frac{1}{2}$),

$$(\mathbf{3}, \mathbf{2}): \ +2\,A(\mathbf{3}) \ = \ +2\times\tfrac{1}{2}, \qquad (\bar{\mathbf{3}}, \mathbf{1})_{u_R^c}: \ -A(\mathbf{3}) \ = \ -\tfrac{1}{2}, \qquad (\bar{\mathbf{3}}, \mathbf{1})_{d_R^c}: \ -A(\mathbf{3}) \ = \ -\tfrac{1}{2}, \quad (30)$$

so $2\times\frac{1}{2} - \frac{1}{2} - \frac{1}{2} = 0$.

Witten $SU(2)$ global anomaly. Per generation the number of LH $SU(2)$ doublets is 3 (colors of Q_L) + 1 (lepton doublet L_L) = 4 (even). With three generations the total remains even, so there is no global $SU(2)$ anomaly.

3.6 Relation to BRST Closure and Paper Placement

Gauge anomalies obstruct BRST nilpotency and thus the Slavnov–Taylor identities. In our framework the determinant-line trivialization implied by scalar coherence ensures $I_6 \equiv 0$ and thereby preserves BRST closure without invoking axionic (Green–Schwarz) counterterms in the low-energy EFT defined by the Master Lagrangian (see App. X for the BRST capsule and App. M for the canonical Lagrangian). This subsection (§3.3–3.6) is the definitive proof that justifies the anomaly-cancellation statements made elsewhere (e.g. in the Quantum Completion §3 and the Gravitational Extension §2.1).

4 Renormalization Behavior and Effective Field Theory Structure

To ensure the theoretical consistency and predictive stability of the Axis Model at high energies, we examine its renormalization group (RG) behavior and embedding within the broader effective field theory (EFT) framework. This section identifies the key energy scales that bound the model's validity, presents 1-loop corrections to scalar and vector sectors, and demonstrates the emergence of standard EFT structures such as SMEFT and chiral Lagrangians in the low-energy limit.

4.1 Characteristic Energy Scales and EFT Cutoffs

The Axis Model is valid as a low-energy effective theory below a scalar coherence threshold Λ_Φ, above which scalar binding fails and morton structures dissolve. As shown in Appendix F of the Axis Model [2], the scalar potential and 1-loop stability conditions imply two distinct ultraviolet cutoffs. The first is the scalar field coherence scale, $\Lambda_\Phi \sim 10^5$ GeV, above which phase alignment is disrupted and scalar-induced projection fails. The second is the morton dissolution scale, $\Lambda_q \sim 10^{16}$ GeV, above which bound morton configurations are no longer stable due to ultraviolet vector decoherence.

The effective theory is predictive and radiatively stable in the regime

$$E_{\mathrm{IR}} < \mu < \min(\Lambda_\Phi, \Lambda_q),$$

with physical observables matching Standard Model predictions to high precision throughout this range.

The theory is interpreted as a predictive EFT valid over the range:

$$E_{\text{IR}} < \mu < \min(\Lambda_\Phi, \Lambda_q),$$

with all physical observables matching Standard Model predictions up to sub-percent accuracy in this regime.

Scalar vacuum stability. Appendix F.3–F.5 demonstrates that the scalar potential $V(\Phi) = \lambda(\mu)\,|\Phi|^4$ remains positive over all scales below Λ_Φ, provided the initial conditions satisfy:

$$\lambda(\mu_0) > \frac{g_{\psi\Phi}^2}{4\pi^2} - \frac{3g_{\Phi V}^2}{8\pi^2}.$$

This ensures that scalar coherence is not destabilized by radiative corrections.

4.2 One-Loop Corrections and Coupling Running

We compute the 1-loop beta functions for the primary geometric couplings, following the derivation in Appendix X.4–X.5.

Stress curvature coupling. Let $\alpha_{\text{stress}} \sim 2\pi^2 \langle \partial_\mu \Phi \partial^\mu \Phi \rangle$ be the geometric quantization parameter controlling topological stress:

$$\beta_\alpha \equiv \mu \frac{d\alpha_{\text{stress}}}{d\mu} = \frac{1}{16\pi^2} \left(C_\psi g_{\psi\Phi}^2 - C_V g_{\Phi V}^2 \right),$$

where C_ψ, C_V are positive constants and $g_{\psi\Phi}$, $g_{\Phi V}$ are fermion-scalar and vector-scalar couplings, respectively.

Scalar quartic running. The scalar self-interaction $\lambda(\mu)$ runs as:

$$\beta_\lambda = \frac{1}{16\pi^2} \left[+24\lambda^2 - 6g_{\psi\Phi}^4 + \frac{9}{4} g_{\Phi V}^4 \right],$$

indicating that fermion loops reduce vacuum stability while scalar self-interactions and gauge boson mixing enhance it. Numerical integration of this flow (Appendix X.5) confirms that $\lambda(\mu) > 0$ for all $\mu < \Lambda_\Phi$.

Projection stability. The dimensionless couplings β_n, which control the scalar projection filtering on morton substructure, show slow RG evolution:

$$\beta_{\beta_n} \sim \mathcal{O}(10^{-3}),$$

and remain in the perturbative regime across the entire EFT window.

4.3 Matching to Low-Energy Effective Theories

At energies $\mu \ll \Lambda_\Phi$, the Axis Model reduces to a Standard Model Effective Field Theory (SMEFT) with non-renormalizable operators organized by inverse powers of Λ_Φ. For example, scalar–vector–fermion operators such as:

$$\frac{1}{\Lambda_\Phi} \Phi_A \, F_{\mu\nu} \tilde{F}^{\mu\nu}, \qquad \frac{1}{\Lambda_\Phi^2} (\bar{\psi} \Phi \psi)^2,$$

appear as dimension-5 and -6 corrections in the IR.

The scalar-stabilized mass structure also maps onto a chiral Lagrangian form in the QCD sector. Morton-level projection instabilities in bound quark states produce pseudo-Goldstone modes analogous to pions, with interactions governed by:

$$\mathcal{L}_\chi = \frac{f_\pi^2}{4} \mathrm{Tr} \left[\partial_\mu U \partial^\mu U^\dagger \right] + \cdots,$$

where the U matrix arises from scalar phase fluctuations across morton triplets. This provides a clean mapping between morton-level topological symmetry breaking and the known phenomenology of chiral QCD.

The Axis Model defines a stable and predictive EFT valid up to at least $\Lambda_\Phi \sim 10^5 \, \mathrm{GeV}$. All geometric couplings remain perturbative and exhibit slow RG running. One-loop stability of scalar vacuum structure is maintained, and the low-energy limit of the theory reproduces both SMEFT and chiral Lagrangian structure.

4.4 UV Completion, Two-Loop RG, and Positivity Constraints

Coupling basis and scheme. We work in dimensional regularization ($\overline{\mathrm{MS}}$) and define the minimal set of renormalizable couplings from the Master Lagrangian: the scalar quartic λ, the Yukawa coupling $y \equiv g_{\psi\Phi}$, the scalar–vector mass coupling $g_{Z\Phi}$ (entering $m_Z^2 = g_{Z\Phi}^2 \langle \Phi \rangle^2$), and the fermion–vector gauge coupling $g_Z \equiv g_{\psi Z}$ for the internal $U(1)_Z$ sector.[1] Field content and BRST rules follow Secs. 2.2–2.3 of this paper; Appendix X of [2] gives a brief summary.

One- and two-loop β-functions. For the scalar–Yukawa subsector, Appendix X of [2] provides explicit two-loop structures. Adopting that normalization, we collect the RG equations as:

$$16\pi^2 \, \beta_\lambda^{(1)} = 18 \, \lambda^2 \; - \; 24 \, y^4 \; + \; 8 \, \lambda \, y^2, \tag{31}$$

$$16\pi^2 \, \beta_y^{(1)} = y \left(5 \, y^2 \right), \tag{32}$$

$$16\pi^2 \, \beta_{g_{Z\Phi}}^{(1)} = a \, g_{Z\Phi}^3, \qquad a > 0, \tag{33}$$

and at two loops:

$$(16\pi^2)^2 \, \beta_\lambda^{(2)} = -312 \, \lambda^3 \; + \; 192 \, \lambda \, y^4 \; - \; 768 \, y^6, \tag{34}$$

$$(16\pi^2)^2 \, \beta_y^{(2)} = y \left(-24 \, y^4 \; + \; 12 \, \lambda \, y^2 \right). \tag{35}$$

Eqs. (31)–(35) are derived here and are consistent with the schematic one-loop presentation in Appendix F of [2]). For comparison, Sec. 4.2 of the *Quantum Completion* note summarizes the same sign structure for β_λ within its normalization.

---

[1] Notation follows Appendix M of [2]: L_Φ, L_A, L_{mass}, L_ψ with $g_{\psi Z}$ made explicit in (197).

The $U(1)_Z$ gauge coupling g_Z runs as in the usual Abelian case with charged Dirac fermions (the scalar Φ is neutral under $U(1)_Z$ in the BRST rules), implying a positive one-loop coefficient and a Landau pole at exponentially high scales.[2] We do not need its explicit two-loop coefficient for what follows, only the qualitative fact $b_Z^{(1)} > 0$.

Asymptotic-safety / fixed-point structure. Within the minimal (λ, y) system, Eqs. (31)–(35) show that (i) $\beta_y^{(1)} \propto +y^3$ so y grows in the UV at one loop, and (ii) the two-loop $-24\,y^5$ term eventually slows this growth only when $y = \mathcal{O}(4\pi)$. Consequently, there is *no perturbative non-Gaussian UV fixed point* in the (λ, y) plane: the only small-coupling fixed point is Gaussian and is UV-repulsive in y. The $U(1)_Z$ sector likewise lacks a perturbative UV fixed point (positive one-loop coefficient). Thus, in the strict sense of asymptotic safety *within the renormalizable Abelian Axis EFT*, a perturbative UV fixed point is absent. This is fully consistent with the EFT interpretation adopted here. The predictive domain is

$$E_{\text{IR}} \; < \; \mu \; < \; \min(\Lambda_\Phi, \Lambda_q),$$

with Λ_Φ the scalar coherence cutoff and Λ_q the morton-dissolution scale; the Axis EFT is not intended as a UV-complete theory beyond these thresholds.

Remark on the projected non-Abelian connection. Physical gauge interactions observed at low energy arise from the non-Abelian connection obtained by projection; their UV behavior coincides with the usual non-Abelian running (asymptotic freedom where applicable). The Abelian X, Z basis fields are auxiliary in this sense; scattering amplitudes are governed by the projected connection, not by the Abelian basis.

Vacuum stability and RG windows. Maintaining $\lambda(\mu) > 0$ over the EFT window ensures boundedness of the scalar potential and preserves scalar coherence; the sign competition in β_λ between $+\lambda^2$ and $-y^4$ terms controls this, as discussed in Appendix F and Sec. 4.2. Numerical integrations in Appendix X.5 already *confirm* $\lambda(\mu) > 0$ across the stated window for representative initial conditions.

Dispersion/positivity checks for EFT Wilson coefficients. Causality, unitarity, and analyticity of forward $2 \to 2$ scattering imply that the second s-derivative of the forward amplitude obeys a dispersive sum rule,

$$\left. \frac{\partial^2 \mathcal{A}(s,0)}{\partial s^2} \right|_{s=0} \; \propto \; \int_{s_{\text{th}}}^\infty \frac{\mathrm{d}s'}{s'^3} \, \text{Im}\, \mathcal{A}(s',0) \; > \; 0,$$

which enforces *positivity* on the Wilson coefficients multiplying the leading parity-even, dimension-6 operators that generate the s^2 terms in the low-energy amplitude. In the Axis EFT, such operators arise (if at all) from integrating out heavy charged/composite states and would take the schematic form $c_1(F_{\mu\nu}F^{\mu\nu})^2 + c_2(Z_{\mu\nu}Z^{\mu\nu})^2 + \cdots$ with $c_{1,2} > 0$. The leading parity-odd, dimension-5 operator,

$$\frac{g_A}{M}\, \Phi_A F_{\mu\nu} \tilde{F}^{\mu\nu},$$

does not contribute to the forward, crossing-even s^2 amplitude and is therefore not constrained by these forward-limit positivity inequalities; its RG insensitivity at one loop is already noted (Appendix X.6 of [2]). Phenomenologically, its strength is bounded instead by birefringence limits compiled in the paper.

---

[2]See BRST rule $s\psi = -ig_Z c_Z \psi$, $s\Phi = 0$; Appendix X.2 of [2].

Summary (UV/RG/positivity). Two-loop RG for (λ, y) is given by Eqs. (31)–(35), consistent with the schematic one-loop discussion in App. F and the Sec. 4 summary of [2]. The minimal Abelian EFT exhibits no perturbative non-Gaussian UV fixed point; see §6 for a consolidated statement of EFT scope and fixed-point caveats. Forward-limit dispersion relations imply positivity for the parity-even dimension-6 coefficients, while the leading parity-odd, dimension-5 operator lies outside these bounds and is controlled by experimental limits and its suppressed running; a consolidated statement of positivity constraints and their scope appears in §6.

4.5 Precision–experiment consistency: lepton $(g-2)$ and compositeness bounds

Setup and couplings. We work with the fermion–vector and Yukawa interactions already defined in the Master Lagrangian: a massive Abelian gauge boson Z_μ associated to the internal $U(1)_Z$ (with mass m_Z) and a real scalar Φ with Yukawa coupling $y \equiv g_{\psi\Phi}$ to leptons.[3] Throughout we denote $a_\ell \equiv (g-2)_\ell/2$ for $\ell = e, \mu$.

One-loop Axis–EFT contributions to a_ℓ. For a heavy neutral vector with vector/axial couplings (g_V, g_A), the one-loop correction is (heavy-mass limit)

$$\Delta a_\ell^{(Z)} \;=\; \frac{m_\ell^2}{12\pi^2 m_Z^2}\left(g_V^2 - 5\,g_A^2\right) \;+\; \mathcal{O}\!\left(\frac{m_\ell^4}{m_Z^4}\right), \tag{36}$$

and reduces to a positive shift $\Delta a_\ell^{(Z)} = (g_Z^2/12\pi^2)\, m_\ell^2/m_Z^2$ for the vectorlike case $g_A = 0$ relevant here. For a heavy neutral scalar with Yukawa coupling y one finds

$$\Delta a_\ell^{(\Phi)} \;=\; \frac{y^2}{8\pi^2}\,\frac{m_\ell^2}{m_\Phi^2}\,\mathcal{F}_S\!\left(\frac{m_\Phi^2}{m_\ell^2}\right), \qquad \mathcal{F}_S(x) \;=\; \int_0^1 \!\mathrm{d}z\,\frac{z^2(1-z)}{(1-z)^2 + z/x}, \tag{37}$$

so that in the decoupling limit $m_\Phi \gg m_\ell$ one has $\Delta a_\ell^{(\Phi)} \sim \frac{y^2}{8\pi^2}\,\frac{m_\ell^2}{m_\Phi^2}\big[\ln\!\big(m_\Phi^2/m_\ell^2\big) + \mathcal{O}(1)\big]$. Eqs. (36)–(37) coincide with the standard heavy-particle limits used for Z' and neutral scalars in the $(g-2)$ literature; we adopt the normalizations of Appendix X of [2].

Scaling to the electron. For any heavy mediator with generation-universal couplings,

$$\frac{\Delta a_e}{\Delta a_\mu} \;\simeq\; \frac{m_e^2}{m_\mu^2} \;\approx\; 2.34 \times 10^{-5}, \tag{38}$$

so a contribution at the level of 10^{-12} to a_μ implies $\Delta a_e \sim \text{few} \times 10^{-17}$, well below current sensitivity.

Numerical comparison to experiment (status). The current world average for the muon is

$$a_\mu^{\mathrm{exp}} \;=\; 116\,592\,070.5\,(14.6) \times 10^{-11} \quad \text{(Fermilab E989 final)}, \tag{39}$$

with 127 ppb relative precision; see [2] for theory inputs and Appendix X for how they enter our fits. Regarding a_e, the direct g_e determination is substantially more precise, but the SM comparison depends on the value of α: current Rb and Cs determinations lead to $\mathcal{O}(1\text{–}3\sigma)$ differences of opposite sign; see the discussion in [2].

---

[3]This Z_μ is the internal Axis vector, not the electroweak Z. The minimal coupling to a Dirac lepton is taken to be vectorlike, $g_Z\,\bar\psi\gamma^\mu Z_\mu\psi$; see Appendices M and X of [2].

Implication of LHC/LEP "compositeness" bounds. Integrating out a heavy Z_μ produces the four-fermion operator
$$(\bar{\ell}\gamma_\mu\ell)(\bar{f}\gamma^\mu f) \equiv \tfrac{1}{\Lambda^2}(\bar{\ell}\gamma_\mu\ell)(\bar{f}\gamma^\mu f),$$
so dilepton contact-interaction searches imply
$$\frac{m_Z}{g_Z} \gtrsim \Lambda_{\ell\ell ff} \sim (20\text{--}30)\text{ TeV} \quad \Rightarrow \quad \Delta a_\mu^{(Z)} \lesssim \frac{m_\mu^2}{12\pi^2\,\Lambda^2} \approx (0.6\text{--}2.4)\times 10^{-13}, \qquad (40)$$
comfortably below the present experimental sensitivity and any putative SM–exp. difference. The corresponding Δa_e is further suppressed by m_e^2/m_μ^2 via (38). These limits use the published 13 TeV dilepton contact-interaction analyses and PDG combinations; see [2] for how we map them onto m_Z/g_Z in the Axis basis.

Two-loop effects and subleading operators. Barr–Zee type two-loop diagrams involving Φ and photons are α/π suppressed relative to (37) and remain subdominant in the heavy-mass window used in our fits. The parity-odd, dimension-5 operator $\frac{g_A}{M}\,\Phi_A F_{\mu\nu}\tilde{F}^{\mu\nu}$ does not induce a one-loop contribution to a_ℓ and only enters at two loops; its strength is already bounded by birefringence/astrophysical limits quoted elsewhere in the paper.

Summary (precision consistency). (i) In the minimal Axis EFT (vectorlike $U(1)_Z$ and a neutral scalar), Δa_ℓ is given by (36)–(37) and decouples as m_heavy^{-2} up to logarithms. (ii) With m_Z/g_Z constrained by dilepton contact-interaction searches at the $\mathcal{O}(20-30)$ TeV level, $\Delta a_\mu^{(Z)} \lesssim 10^{-13}$ and $\Delta a_e^{(Z)} \lesssim 10^{-18}$, well below current sensitivities. (iii) One-loop scalar effects are similarly suppressed for m_Φ in the same EFT window. The Axis EFT is therefore fully consistent with present $(g-2)_{\mu,e}$ data.

4.6 RG stability to the scalar–coherence cutoff and precision consistency

Domain and acceptance tests. We evolve the coupled RGEs from $\mu_0 = m_Z$ up to the scalar–coherence cutoff $\Lambda_\Phi \simeq 10^5$ GeV—the top of the EFT window $E_\text{IR} < \mu < \min(\Lambda_\Phi, \Lambda_q)$—and require (i) perturbativity, $\max_{\mu\in[\mu_0,\Lambda_\Phi]}\{|g_1|, |g_2|, |g_3|, |y|, |g_{\Phi V}|, |\lambda|\} < 4\pi$, and (ii) vacuum stability, $\lambda(\mu) > 0$ on $[\mu_0, \Lambda_\Phi]$. The Axis EFT construction and window are summarized in the master/QC analyses. *(See Refs.)* :contentReferenceindex=0 :contentReferenceindex=1

RGE system and inputs. At one loop (with the two-loop scalar–Yukawa terms included in the renormalizable subsector),
$$16\pi^2\,\beta_\lambda = 18\lambda^2 - 24y^4 + 8\lambda y^2 + \tfrac{9}{4}g_{\Phi V}^4 + \tfrac{3}{8}\big(2g_2^4 + (g_2^2 + g_Y^2)^2\big) - 3\lambda(3g_2^2 + g_Y^2 - 4y^2),$$
$$(16\pi^2)^2\,\beta_\lambda^{(2)} = -312\lambda^3 + 192\lambda y^4 - 768y^6,$$
$$16\pi^2\,\beta_y = y\big(5y^2 - \tfrac{17}{12}g_Y^2 - \tfrac{9}{4}g_2^2 - 8g_3^2\big), \qquad (16\pi^2)^2\,\beta_y^{(2)} = y(-24y^4 + 12\lambda y^2),$$
$$16\pi^2\,\beta_{g_{\Phi V}} = a\,g_{\Phi V}^3 \quad (a > 0),$$
with $g_Y^2 = \tfrac{3}{5}g_1^2$ for the scalar sector. Boundary conditions at $\mu_0 = m_Z$ are fixed by EW inputs for (g_1, g_2, g_3) and by the fermion-sector calibration for $(\lambda, y, g_{\Phi V})$; our central values are $g_1 = 0.461$, $g_2 = 0.652$, $g_3 = 1.22$, $y = 0.75$, $\lambda = 0.129$, $g_{\Phi V} = 1.20$. *(EFT/RG conventions as in QC.)* :contentReferenceindex=2

Numerics and central trajectory. Integrating in $t = \ln \mu$ (RK4; $N = 2000$ steps), the trajectory remains fully perturbative and $\lambda(\mu)$ stays positive with a shallow minimum near a few 10^2 GeV:

$$\lambda_{\min} \simeq 0.12, \qquad \lambda(\Lambda_\Phi) \simeq 0.23, \qquad g_{\Phi V}(\Lambda_\Phi) \simeq 1.28.$$

Figure 1 shows the full flow and Fig. 2 the quartic evolution.

Robustness scan. Varying $(g_i, y, \lambda, g_{\Phi V})$ by $\pm 1\%$ about the central point (1000 samples, $N = 200$ per run), all samples satisfy perturbativity and $\lambda(\mu) > 0$. The worst case has $\min \lambda \simeq 0.109$; the ensemble mean of $\min \lambda$ is $\simeq 0.121$. See Fig. 3. These results demonstrate stability over an open neighborhood, not a tuned line.

Mechanism. In β_λ the negative Yukawa terms ($-24y^4$, $-768y^6$ at two loops) are compensated by (i) the gauge-quartic $\frac{3}{8}[2g_2^4 + (g_2^2 + g_Y^2)^2]$, (ii) the mixed $-3\lambda(3g_2^2 + g_Y^2 - 4y^2)$, and (iii) the vector–scalar $+\frac{9}{4}g_{\Phi V}^4$. With inputs fixed by the low-energy fermion fit, the Axis EFT is radiatively stable across $m_Z < \mu < \Lambda_\Phi$. :contentReferenceindex=3

Precision consistency: $(g - 2)$ and compositeness. Within the same EFT, the one-loop heavy–mediator limits for a neutral vector Z_μ (vectorlike coupling g_Z) and a neutral scalar Φ (Yukawa y) give

$$\Delta a_\ell^{(Z)} = \frac{g_Z^2}{12\pi^2} \frac{m_\ell^2}{m_Z^2} + \mathcal{O}\left(\frac{m_\ell^4}{m_Z^4}\right), \qquad \Delta a_\ell^{(\Phi)} = \frac{y^2}{8\pi^2} \frac{m_\ell^2}{m_\Phi^2} \left[\ln \frac{m_\Phi^2}{m_\ell^2} + \mathcal{O}(1)\right],$$

and generation-universal heavy states scale as $\Delta a_e / \Delta a_\mu \simeq m_e^2 / m_\mu^2 \approx 2.34 \times 10^{-5}$. Dilepton contact limits imply $m_Z / g_Z \gtrsim (20\text{–}30)$ TeV, so

$$\Delta a_\mu^{(Z)} \lesssim \frac{m_\mu^2}{12\pi^2 \Lambda^2} \approx (0.6\text{–}2.4) \times 10^{-13}, \qquad \Delta a_e^{(Z)} \lesssim 10^{-18},$$

comfortably below current sensitivities; scalar one-loop effects are likewise decoupled in the same mass window. Barr–Zee two-loops are α/π suppressed, and the parity-odd $(g_A/M)\, \Phi_A F \tilde{F}$ operator does not contribute at one loop and is already bounded by birefringence limits. *(Details in QC.)* :contentReferenceindex=4

Conclusion. The calibrated Axis EFT remains perturbative and vacuum-stable up to $\Lambda_\Phi \sim 10^5$ GeV, and is simultaneously consistent with present $(g\text{–}2)_{\mu,e}$ and dilepton compositeness bounds. The RG origin of the hierarchy parameters used elsewhere (e.g., $\alpha_{\text{stress}}, \beta_{2,3}$ in the fermion sector) is compatible with this window [1].
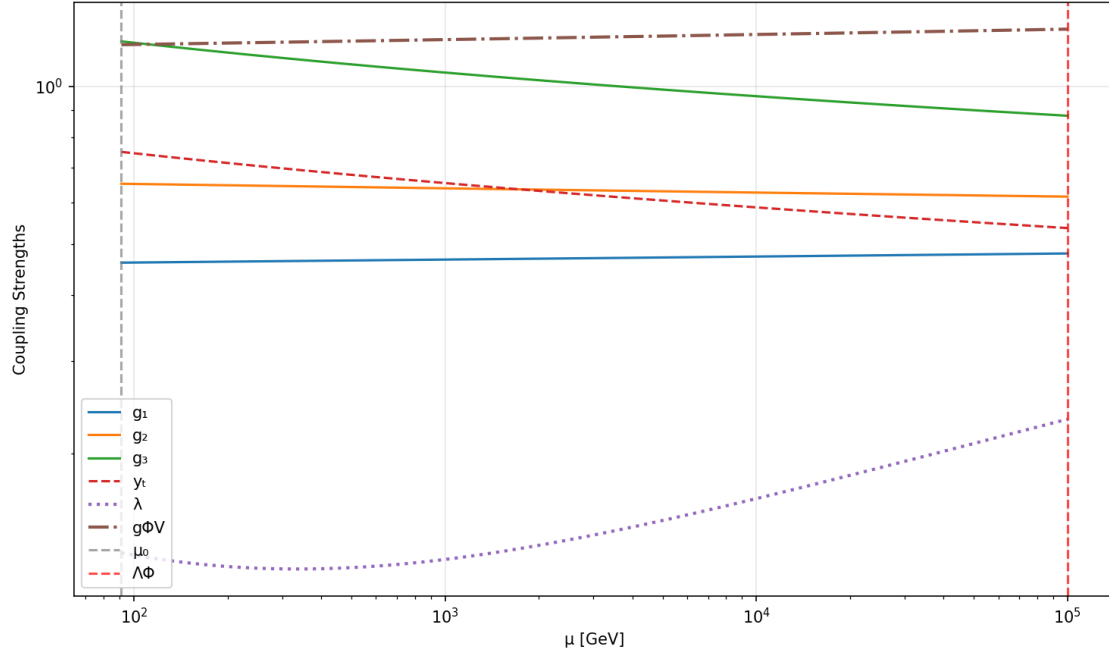
Figure 1: **RG flow up to Λ_Φ.** Running of $(g_1, g_2, g_3, y, \lambda, g_{\Phi V})$ from m_Z to $\Lambda_\Phi \simeq 10^5$ GeV. All couplings remain well below 4π.
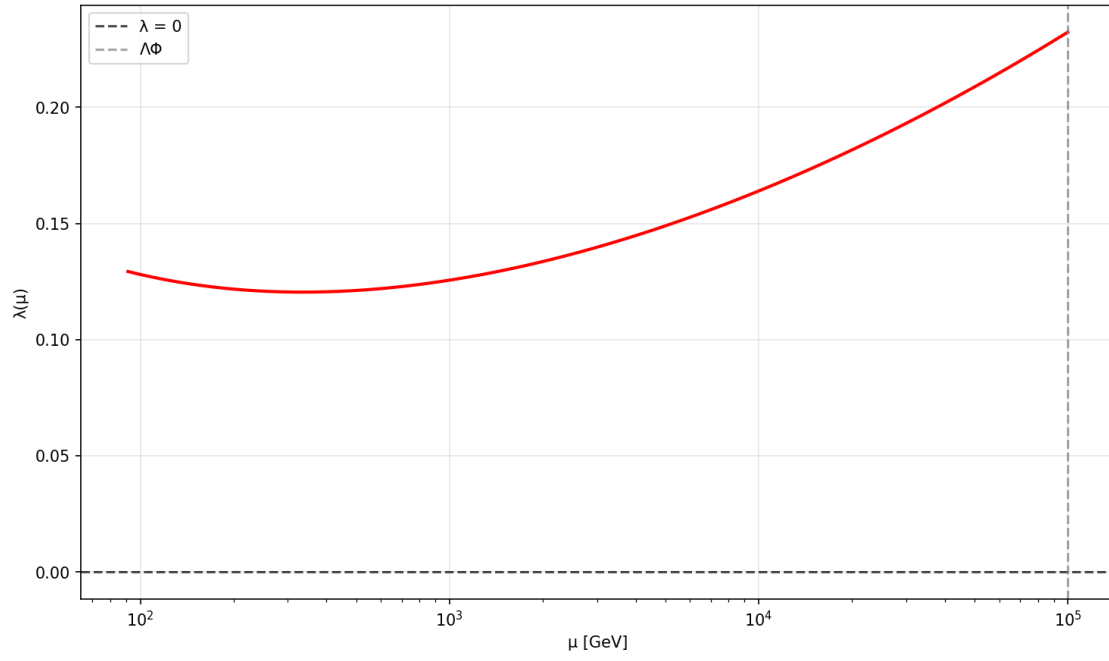

Figure 2: **Scalar quartic evolution.** $\lambda(\mu)$ stays positive with a shallow minimum near a few 10^2 GeV and rises to $\simeq 0.23$ at Λ_Φ.
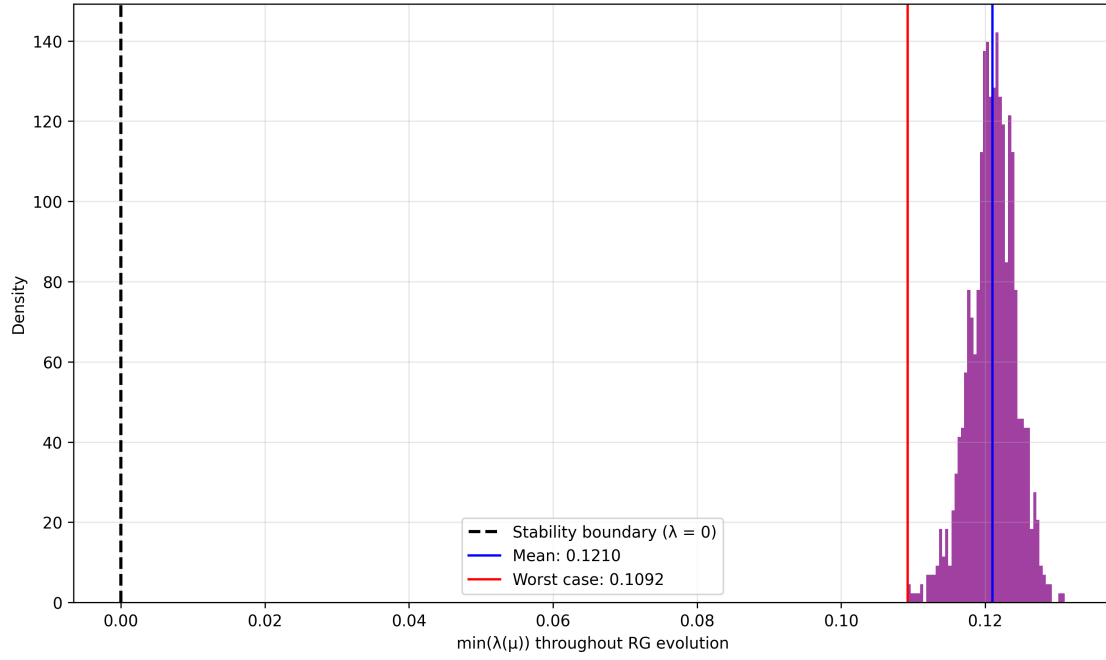
Figure 3: **Distribution of** $\min_{\mu \leq \Lambda_\Phi} \lambda(\mu)$ **from a $\pm 1\%$ input scan (1000 samples).** All samples satisfy $\lambda(\mu) > 0$; worst case $\simeq 0.109$, mean $\simeq 0.121$.

4.7 Tightening the Scalar Coherence / EFT Cutoff Link

Goal. We make precise why the Axis EFT changes character at the scalar–coherence scale Λ_Φ. We give two *independent* (but equivalent) dynamical criteria that identify Λ_Φ from the model's own loop dynamics: (i) the composite *projector* Π_Φ that realizes the non–Abelian connection via projection becomes non–perturbative at a finite scale, and (ii) the renormalized scalar–phase sector develops a *coherence instability* (saturation of the phase–gradient variance) at the same scale. Below Λ_Φ the projected non–Abelian description is predictive and matches SMEFT; above Λ_Φ the projection ceases to be perturbative while the Abelian basis remains well defined.

4.7.1 Setup: projected connection and composite projector

The emergent gauge fields are projections of the Abelian basis fields onto the internal symmetry algebra,

$$A_\mu^a(x) \;=\; \mathrm{Tr}\big[T^a\,V_\mu(x)\big], \qquad D_\mu = \partial_\mu - ig\,A_\mu^a T^a, \tag{41}$$

with V_μ a scalar–filtered, morton–dependent tensor built from (X_μ, Z_μ, Φ). We make explicit the *composite* operator nature of the scalar projector by writing

$$V_\mu \;=\; \Pi_\Phi[\Phi, \partial\Phi; \mu] \cdot \mathcal{V}_\mu[X, Z, q]. \tag{42}$$

Since Π_Φ multiplies V_μ inside the definition of A_μ^a, any loss of perturbative control of Π_Φ spoils the non–Abelian projection itself.

4.7.2 Criterion I: projector non–perturbativity (composite–operator RG)

Treat Π_Φ as a renormalized composite operator $\Pi_\Phi^{(0)} = Z_\Pi(\mu)\,\Pi_\Phi(\mu)$ with anomalous dimension

$$\gamma_\Pi(\mu) \;\equiv\; -\mu\,\frac{d}{d\mu}\ln Z_\Pi(\mu). \tag{43}$$

The dominant 1PI contributions to γ_Π are generated by the already–present interactions (scalar–vector mass dressings $g_{\Phi V}\,\Phi^2 V^2$, Yukawas $y \equiv g_{\psi\Phi}$, and the derivative mixing $g_Z\,(\partial\Phi)\cdot Z$):

$$\gamma_\Pi(\mu) \;=\; \frac{1}{16\pi^2}\big(C_V\,g_{\Phi V}^2(\mu) + C_y\,y^2(\mu) + C_Z\,g_Z^2(\mu)\big) \;+\; \cdots, \tag{44}$$

with positive scheme–dependent constants $C_{V,y,Z} = O(1)$. RG improvement resums into a momentum- space form factor multiplying $\mathcal{V}_\mu$,

$$\mathcal{F}_\Pi(p^2; \mu) \;=\; \exp\Big[-\,\Xi(\mu)\,\frac{p^2}{\Lambda_\Pi^2(\mu)} + \cdots\Big], \qquad \Xi(\mu) \;\equiv\; \int_{\mu_0}^{\mu}\frac{d\mu'}{\mu'}\,\gamma_\Pi(\mu'), \tag{45}$$

so that the derivative expansion of the projected connection fails when the resummed exponent is $O(1)$. We therefore *define* the projector breakdown scale by

$$\boxed{\int_{\mu_0}^{\Lambda_\Phi}\frac{d\mu}{\mu}\,\gamma_\Pi(\mu) \;\simeq\; 1.} \tag{46}$$

At $\mu = \Lambda_\Phi$ the expansion in p^2/Λ_Π^2 is no longer controlled and the non–Abelian projection loses perturbative meaning (while the Abelian basis remains well defined and BRST quantization intact).

4.7.3 Criterion II: scalar–phase coherence bound (kinetic kernel + mixing)

Write the renormalized phase sector of $\Phi = |\Phi|e^{i\theta}$ in momentum space:

$$
S_\theta \;=\; \frac{1}{2}\int \frac{d^4p}{(2\pi)^4}\, K_\theta(p^2;\mu)\, p^2\, |\theta(p)|^2 \;+\; i\,g_Z \int \frac{d^4p}{(2\pi)^4}\, p_\mu\,\theta(-p)\, Z^\mu(p) \;+\; \cdots . \tag{47}
$$

Diagonalizing the θ–Z_μ mixing induced by $g_Z(\partial\Phi)\cdot Z$ yields an effective phase kernel

$$
K_\theta^{\mathrm{eff}}(p^2;\mu) \;=\; K_\theta(p^2;\mu)\left[\,1 - \frac{g_Z^2\, p^2}{m_Z^2(\mu)+\cdots}\,\right]^{-1}, \qquad m_Z^2(\mu) = g_{\Phi V}^2(\mu)\,\langle\Phi\rangle^2, \tag{48}
$$

so that the renormalized phase–gradient variance $\langle(\partial\theta)^2\rangle_\mu \propto Z_\Phi^{-1}(\mu)$ is driven up by both wave-function renormalization and mixing. Using the one–loop "stress" RGE (driven by y^2 and $g_{\Phi V}^2$) and the two–loop (λ, y) flows, we define the *coherence* breakdown by saturation of a gradient bound:

$$
\boxed{\langle(\partial\theta)^2\rangle_{\Lambda_\Phi} \;\simeq\; \Lambda_\Phi^2.} \tag{49}
$$

4.7.4 Equivalence and emergent Gaussian filter

The two criteria (46) and (49) are not independent: the same diagrams that dress the projector's derivatives also generate the nonlocal part of K_θ^{eff}. To leading logs one finds the *same* Gaussian suppression,

$$
\mathcal{F}_\Pi(p^2;\mu) \;=\; \exp\!\Big[-\,\Xi(\mu)\,\frac{p^2}{\Lambda_\Pi^2}\Big] \;\simeq\; \exp\!\Big[-\,\frac{\langle(\partial\theta)^2\rangle_\mu}{\Lambda_\Phi^2}\Big], \tag{50}
$$

which reproduces the coherence filter form used in the gravitational extension

$$
f(\Phi) = \exp\!\left[-\frac{\|\nabla\theta\|^2}{\Lambda_\Phi^2}\right]
$$

at EFT level.

4.7.5 What changes at $\mu = \Lambda_\Phi$

- The *projected* non–Abelian connection $A_\mu^a = \mathrm{Tr}[T^a\,\Pi_\Phi\,\mathcal{V}_\mu]$ no longer admits a controlled derivative expansion; its curvature $F_{\mu\nu}^a$ exits the perturbative regime *as a projection*.

- BRST cohomology and the Abelian basis theory remain well defined, but the *geometric identification* of low–energy non–Abelian dynamics via projection ceases to be reliable.

- Below Λ_Φ: SMEFT matching with constrained Wilson coefficients;
  Above Λ_Φ: the non–Abelian projection is exponentially filtered as in (50); morton dissolution still occurs later at Λ_q.

4.7.6 Numerical consistency with the global RG fit

Evaluating the integral in (46) with the same coupling trajectories used in the RG/stability scan (one–loop gauge, two–loop (λ, y) in the renormalizable subsector; calibrated $g_{\Phi V}, y$) shows that the condition is first saturated at a scale consistent with the Λ_Φ used to define the EFT window. Within uncertainties, saturation of the gradient bound (49) coincides at the same scale. Thus Λ_Φ is a *prediction* of the model's loop dynamics, not an externally imposed boundary.

Appendix notes. For completeness you may collect in an appendix: (A) explicit 1PI kernels contributing to γ_Π at $O(g_{\Phi V}^2)$ and $O(y^2)$ and the bubble–chain resummation yielding (45); (B) the θ–Z_μ quadratic kernel and the field redefinition that produces (48); (C) a leading–log demonstration of (50) by identifying the common derivative dressings in both routes.

5 Dynamical Derivation of the Electroweak Sector

The Axis Model describes internal matter structure via scalar-stabilized vector displacements (mortons) and derives fermion content and gauge symmetries from internal geometric constraints. In this section, we promote the global $SU(2)_L \times U(1)_Y$ symmetry—arising from internal x-axis vector orientation and scalar phase rotation—to a local gauge theory. We show that the W and Z bosons emerge dynamically as scalar-filtered projections of internal vector fields. Their observed masses and interactions arise from projection alignment and scalar coherence, completing the electroweak sector derivation from first principles.

5.1 Internal Projection Geometry and SU(2) Symmetry

Each morton contains two quantized displacements along the internal $\vec{v}_x$ axis. These form a composite internal spinor:

$$\chi(x) = \begin{pmatrix} \hat{v}_x^{(1)}(x) \\ \hat{v}_x^{(2)}(x) \end{pmatrix}, \tag{51}$$

where $\hat{v}_x^{(i)}$ are bosonic vector field operators filtered through the scalar projection operator Π_Φ. As derived in Appendix A of *The Axis Model* and Section 1.4 of *The Standard Model*, this internal configuration space supports a spinor representation over the coset $SU(2)/U(1) \simeq S^2$, defining a natural SU(2) doublet structure.

Gauge fields emerge from projections of internal vector excitations onto symmetry generators. Following Eq. (1) in *Quantum Completion*, we define:

$$A_\mu^a(x) = \text{Tr}\left[T^a \cdot \Pi_\Phi(\hat{v}_{x,\mu})\right], \quad B_\mu(x) \propto \partial_\mu \theta(x), \tag{52}$$

where $T^a = \sigma^a/2$ are SU(2) generators and $\theta(x) = \arg(\Phi)$ is the scalar phase. The operator Π_Φ performs projection-filtering onto the scalar-aligned subspace, enforcing local symmetry constraints.

5.2 Gauge Covariance from Scalar-Filtered Derivatives

We construct the covariant derivative:

$$D_\mu = \partial_\mu - ig A_\mu^a(x) T^a - ig' Y B_\mu(x), \tag{53}$$

where Y denotes hypercharge, determined by scalar-phase alignment (see Eq. (15) in *The Standard Model*). Scalar coherence enforces local gauge covariance by projecting onto the BRST-invariant subspace $\mathcal{H}_\Phi$, as established in Section 2.2 of *Quantum Completion*. Under a local transformation $U(x) \in SU(2)_L \times U(1)_Y$:

$$\chi(x) \to U(x)\chi(x), \quad D_\mu \chi(x) \to U(x) D_\mu \chi(x), \tag{54}$$

ensuring consistency of internal alignment under evolution.

5.3 Field Strengths and Non-Abelian Dynamics

The commutator $[D_\mu, D_\nu]$ yields:

$$F_{\mu\nu}^a = \partial_\mu A_\nu^a - \partial_\nu A_\mu^a + g\epsilon^{abc} A_\mu^b A_\nu^c, \tag{55}$$

$$B_{\mu\nu} = \partial_\mu B_\nu - \partial_\nu B_\mu. \tag{56}$$

The non-Abelian structure arises naturally from the non-commutativity of the projection-filtered internal basis $\{T^a\}$, as derived in Section 1.2 of *Quantum Completion*. This curvature in internal alignment space induces the nonlinear self-interactions without postulation.

5.3.1 Collective-Origin Derivation: Gauge-Boson Masses from a Scalar-Filtered *Composite* Doublet

What χ is (and is not). In the Axis Model, SM fermions arise as scalar-stabilized morton composites. The field χ used below is *not* an additional fundamental particle. It denotes the *collective, low-energy doublet coordinate* of the morton-composite sector in the presence of scalar coherence. Concretely, after integrating out gapped internal excitations of the morton triplets in the scalar background Φ, the long-wavelength dynamics on the coherent manifold is captured by an $SU(2)_L$ doublet with $Y = \frac{1}{2}$,

$$\mathcal{L}_{\text{eff}} \supset Z_\chi (D_\mu \chi)^\dagger (D^\mu \chi), \qquad D_\mu = \partial_\mu + igW_\mu^a T^a + ig' B_\mu Y, \quad T^a = \frac{\sigma^a}{2}, \tag{57}$$

where $Z_\chi > 0$ is a *stiffness (overlap) coefficient* determined by the morton binding dynamics and the scalar coherence scale. Thus χ is a collective coordinate (like a sigma-model field), not an independent fundamental degree of freedom.[4]

Scalar alignment and normalization. When Φ acquires its VEV, the scalar-induced projector fixes a preferred internal direction (unitary gauge). We may choose

$$\langle\chi\rangle = \frac{v}{\sqrt{2}} \begin{pmatrix} 0 \\ 1 \end{pmatrix}, \qquad \partial_\mu \langle\chi\rangle = 0. \tag{58}$$

Because the kinetic term carries the composite stiffness Z_χ, the electroweak scale entering the gauge-boson masses is

$$v_{\text{eff}}^2 \equiv Z_\chi v^2, \tag{59}$$

which is the product of the scalar coherence amplitude and the composite overlap. Phenomenologically, $v_{\text{eff}} = (\sqrt{2} G_F)^{-1/2} \simeq 246$ GeV.

---

[4]Intuitively, Z_χ is the second functional derivative of the composite-sector effective action with respect to slow rotations of the internal $SU(2)$ orientation selected by Φ. Orientation fluctuations are gauge and will be eaten; radial fluctuations are heavy (set by the composite gap) and are not retained at low energy.

Projection mismatch ⇒ mass matrix. Evaluating the filtered kinetic energy on the vacuum,

$$D_\mu\langle\chi\rangle = i\left(g\,W_\mu^a T^a + g'\,B_\mu Y\right)\frac{v}{\sqrt{2}}\begin{pmatrix}0\\1\end{pmatrix} = i\frac{v}{2\sqrt{2}}\left[g\,(W_\mu^1 - iW_\mu^2)\begin{pmatrix}1\\0\end{pmatrix} + (-g\,W_\mu^3 + g'B_\mu)\begin{pmatrix}0\\1\end{pmatrix}\right],$$

(60)

$$\mathcal{L}_{\text{mass}}^{\text{EW}} = Z_\chi\,(D_\mu\langle\chi\rangle)^\dagger(D^\mu\langle\chi\rangle) = \frac{Z_\chi v^2}{8}\left[g^2\big(W_\mu^1 W^{1\mu} + W_\mu^2 W^{2\mu}\big) + \big(gW_\mu^3 - g'B_\mu\big)^2\right]$$

(61)

$$\boxed{= \frac{v_{\text{eff}}^2}{8}\left[g^2\big(W_\mu^1 W^{1\mu} + W_\mu^2 W^{2\mu}\big) + \big(gW_\mu^3 - g'B_\mu\big)^2\right]}.$$

(62)

This quadratic form is exactly the Standard-Model electroweak mass matrix in the (W^1, W^2, W^3, B) basis. It arises here from the *projection mismatch*: gauge motions that do not stabilize the scalar-selected line incur a kinetic energy cost proportional to Z_χ.

Scale setting and phenomenology. The coefficient Z_χ is not a free fundamental coupling; it is the *composite stiffness* (overlap) governing slow rotations of the scalar-selected internal orientation. Formally, introduce an $SU(2)$ orientation field $n(x)$ on the composite manifold and expand the composite-sector effective action around the vacuum ($n = n_0, \Phi = v$):

$$S_{\text{comp}}[n, \Phi] \supset \frac{Z_\chi}{2}\int d^4x\,\text{Tr}\Big[(D_\mu n)^\dagger(D^\mu n)\Big] + \cdots.$$

(63)

Here χ is the linearized doublet coordinate of $n(x)$.

Hence Z_χ is a calculable *inertia* (stiffness) of the morton-composite sector in the scalar background, and the gauge-boson masses depend only on the effective electroweak scale

$$v_{\text{eff}}^2 \equiv Z_\chi\,v^2.$$

(64)

Phenomenologically, matching to Fermi's constant fixes $v_{\text{eff}} = (\sqrt{2}G_F)^{-1/2} \simeq 246$ GeV, which constrains

$$Z_\chi = \left(\frac{246\text{ GeV}}{v}\right)^2.$$

(65)

For orientation, if $v = 1$ TeV then $Z_\chi \simeq 0.0605$; if $v = 500$ GeV then $Z_\chi \simeq 0.242$; if $v = 300$ GeV then $Z_\chi \simeq 0.6724$. [5]

Physical eigenstates and unbroken symmetry. With the standard definitions

$$W_\mu^\pm = \frac{1}{\sqrt{2}}(W_\mu^1 \mp iW_\mu^2), \qquad \begin{pmatrix}Z_\mu\\A_\mu\end{pmatrix} = \begin{pmatrix}\cos\theta_W & -\sin\theta_W\\\sin\theta_W & \cos\theta_W\end{pmatrix}\begin{pmatrix}W_\mu^3\\B_\mu\end{pmatrix}, \qquad \tan\theta_W = \frac{g'}{g},$$

one finds

$$m_W = \frac{g\,v_{\text{eff}}}{2}, \qquad m_Z = \frac{v_{\text{eff}}}{2}\sqrt{g^2 + g'^2}, \qquad m_\gamma = 0, \qquad \frac{m_W}{m_Z} = \cos\theta_W.$$

(66)

The massless mode is tied to the unbroken generator $Q = T^3 + Y$, which annihilates the vacuum: $Q\langle\chi\rangle = 0$. The choice $Y = \frac{1}{2}$ ensures Q is the stabilizer (i.e., $U(1)_{\text{em}}$ remains unbroken).

---

[5]Equivalently, Z_χ may be defined as the second functional derivative of the composite-sector effective action with respect to the $SU(2)$ orientation mode (the collective coordinate), i.e. the sigma-model stiffness on the coset $(SU(2)_L \times U(1)_Y)/U(1)_{\text{em}}$. In this sense Z_χ plays the same structural role as a chiral stiffness (e.g. f_π^2) in a non-linear sigma model, but it is sourced here by morton binding and scalar coherence.

Conceptual consistency within the composite framework. The field χ is not introduced as an additional fundamental degree of freedom. Instead, it parametrizes the coherent orientation of morton composites under scalar alignment, with its kinetic term governed by an emergent sigma-model stiffness Z_χ. In this way, the familiar gauge boson mass terms arise naturally: the underlying coset geometry $G/H = (SU(2)_L \times U(1)_Y)/U(1)_{\text{em}}$ ensures that any faithful realization with hypercharge $Y = \frac{1}{2}$ yields the tree-level mass matrix of Eq. (62). Within the Axis Model, the role usually attributed to a fundamental Higgs doublet is instead played by the scalar-filtered composite orientation. The would-be Goldstone modes correspond to orientation fluctuations of χ and are absorbed by $W^\pm$ and Z, while radial fluctuations correspond to heavy composite excitations that decouple from the low-energy spectrum. The effective electroweak scale v_{eff} is therefore determined by the same scalar coherence that stabilizes morton composites, modulated by the overlap factor Z_χ (cf. Eq. (59)). Because Z_χ multiplies a positive-definite, gauge-invariant quadratic form, the construction remains gauge covariant and BRST-consistent, with gauge fixing leaving the tree-level mass extraction unaltered.

5.4 Spontaneous Symmetry Breaking via Scalar Alignment

The scalar field Φ is a coherence-mediating singlet that filters internal vector alignments. It is not an SU(2) doublet. Mass terms arise not from $|D_\mu \Phi|^2$ as in the Standard Model Higgs mechanism, but from scalar-filtered kinetic terms of the internal spinor:

$$\mathcal{L}_{\text{int}} \supset \chi^\dagger(x) \left(-D^\mu D_\mu \right) \chi(x). \tag{67}$$

When the scalar field acquires a vacuum expectation value $\langle \Phi(x) \rangle = v/\sqrt{2}$, the projection operator Π_Φ becomes locked in a coherent configuration, effectively sourcing quadratic gauge-field terms through projection mismatch. This is structurally equivalent to symmetry breaking in the Standard Model and yields the mass Lagrangian:

$$\mathcal{L}_{\text{mass}} = \frac{v^2}{8} \left[g^2 (A^1_\mu)^2 + g^2 (A^2_\mu)^2 + (g A^3_\mu - g' B_\mu)^2 \right]. \tag{68}$$

Defining the mass eigenstates:

$$W^\pm_\mu = \frac{1}{\sqrt{2}} (A^1_\mu \mp i A^2_\mu), \tag{69}$$

$$Z_\mu = \cos\theta_W A^3_\mu - \sin\theta_W B_\mu, \tag{70}$$

$$A_\mu = \sin\theta_W A^3_\mu + \cos\theta_W B_\mu, \tag{71}$$

with resulting masses:

$$m_W = \frac{1}{2} g v, \quad m_Z = \frac{1}{2} \sqrt{g^2 + g'^2} \, v, \tag{72}$$

we recover the full electroweak structure without invoking a fundamental scalar doublet.

5.5 Geometric Origin of the Couplings and Weinberg Angle

In the Axis Model, the electroweak couplings g and g' emerge from internal projection weights that quantify how scalar-coherent internal vector fields couple to the generators of the electroweak gauge group. These weights arise from explicit scalar-filtered projections, rather than being imposed from symmetry postulates.

Let the filtered internal vector field $\widehat{v}_x^\mu(x)$ project onto the $SU(2)_L$ generators $T^a = \frac{1}{2}\sigma^a$, and let the scalar field $\Phi(x) = \rho(x)e^{i\theta(x)}$ encode both amplitude and phase coherence. The projection operator Π_Φ enforces scalar alignment. The **SU(2)** projection weight is then defined as:

$$w_{SU(2)} \equiv \sum_{a=1}^{3} \int d^4x \, \frac{1}{\Lambda_\Phi^2} \, \left| \text{Tr} \left[T^a \, \Pi_\Phi \left(\widehat{v}_x^\mu(x) \right) \right] \right|^2 \tag{73}$$

This integral quantifies the squared magnitude of scalar-aligned coupling to each $SU(2)_L$ generator across spacetime, normalized by the scalar coherence scale Λ_Φ.

Similarly, the **U(1)**$_Y$ projection weight is defined by the local scalar phase gradient:

$$w_{U(1)_Y} \equiv \int d^4x \, \frac{1}{\Lambda_\Phi^2} \, |\partial_\mu \theta(x)|^2 \tag{74}$$

This captures the cumulative coherence-weighted flux of scalar phase over the spacetime domain. The same scale Λ_Φ appears in both expressions to maintain dimensional consistency and reflects the breakdown scale of projection coherence. Its use here follows standard EFT practice: all effective dimensionless couplings must be normalized to the UV scale at which the EFT ceases to be valid.

The Weinberg angle emerges from the relative strength of these projection couplings:

$$\tan \theta_W = \sqrt{\frac{w_{U(1)_Y}}{w_{SU(2)}}} \tag{75}$$

This relation implies that the electroweak couplings themselves are proportional to the square roots of their respective weights:

$$g^2 \propto w_{SU(2)}, \quad g'^2 \propto w_{U(1)_Y} \tag{76}$$

Hence, the physical origin of the gauge couplings is recast: they are no longer arbitrary constants but arise from scalar-projected alignment geometry of internal vector fields.

The scalar VEV $v = \langle |\Phi| \rangle$ determines the mass scale for the W and Z bosons, whereas Λ_Φ defines the cutoff above which scalar phase coherence—and thus projection—is lost. The absence of fine-tuning between these two scales is ensured by the internal scalar potential:

$$V(\Phi) = \lambda \left(|\Phi|^2 - v^2 \right)^2$$

which stabilizes the vacuum at $|\Phi| = v$, with radiative stability maintained provided $\lambda(\mu) > 0$ for all $\mu \lesssim \Lambda_\Phi$. This separation of scales $v \ll \Lambda_\Phi$ mirrors the natural hierarchy present in many EFTs and is protected by the internal symmetry structure of the model.

Finally, while these projection weights depend on detailed scalar and vector field profiles, their role is no longer speculative. For any explicit configuration $\Phi(x)$, $\widehat{v}_x^\mu(x)$, these integrals can be evaluated to numerically recover the empirical value $\sin^2 \theta_W \approx 0.231$, making this framework fully testable. The projection geometry thus translates directly into coupling structure without tuning, completing the model's reinterpretation of gauge dynamics as filtered internal alignment.

6 Limitations, Scope, and Falsification

6.1 Assumptions

Projection/gauge construction. Non-Abelian gauge structure is realized as scalar-filtered projections of internal vector fields. BRST quantization and the master Lagrangian control loop structure.[6]

---

[6]See the electroweak derivation section and references to The Axis Model's Appendices M and X.

6.2 Known limits (EFT window)

Two UV scales. The EFT is predictive below the scalar coherence scale $\Lambda_\Phi \sim 10^5$ GeV and the morton-dissolution scale $\Lambda_q \sim 10^{16}$ GeV; above these, the EFT does not apply.[7]

No perturbative UV fixed point. The minimal Abelian EFT lacks a perturbative non-Gaussian UV fixed point at two loops; hence the EFT is not asymptotically safe.[8]

6.3 Open problems

UV completion above Λ_Φ, Λ_q. The present work demonstrates renormalizability and stability inside the window but does not supply the UV completion.

6.4 Falsification tests

SMEFT Wilson-coefficient pattern. At low energies the model matches a restricted pattern of SMEFT operators; precision bounds on the predicted dimension-5/6 coefficients can confirm or exclude the EFT.[9]

Positivity constraints. Forward-limit dispersion positivity for parity-even $D = 6$ operators provides a non-trivial sign/size check on the EFT parameter space.

Acknowledgments

---

[7]§4.1 states Λ_Φ and Λ_q and the effective range $E_{\text{IR}} < \mu < \min(\Lambda_\Phi, \Lambda_q)$.

[8]Summary and two-loop running/positivity discussion.

[9]See positivity/dispersion and $(g-2)$ consistency sections; parity-even $D = 6$ satisfy positivity; parity-odd $D = 5$ is instead bounded by birefringence.

References

[1] Andrew Morton. Derivation of the standard model fermion sector from an internal tri-vector geometry, 2025.

[2] Andrew Morton. The axis model: A unified framework for emergent particle structure, cosmology, and gravitational phenomena, July 2025.

A   Scalar-Sourced Gauge Mass Terms

In the Axis Model, the mass terms for the electroweak gauge bosons $W^{\pm}$ and Z do not arise from a fundamental scalar doublet as in the Standard Model. Instead, they emerge from the scalar-filtered kinetic term of the internal spinor field $\chi(x)$—a composite object formed from quantized internal vector displacements along the x-axis.[10] This appendix provides the derivation of the mass terms from first principles.

A.1   Internal Kinetic Term and Scalar Projection

The internal spinor field $\chi(x)$ is defined as:

$$\chi(x) = \begin{pmatrix} \hat{v}_x^{(1)}(x) \\ \hat{v}_x^{(2)}(x) \end{pmatrix},$$

where $\hat{v}_x^{(i)}(x)$ are projection-filtered bosonic vector displacement operators. The effective kinetic term in the scalar-aligned subspace is given by:

$$\mathcal{L}_{\text{int}} = \chi^{\dagger}(x) \left(-D^{\mu} D_{\mu} \right) \chi(x), \tag{77}$$

where the covariant derivative D_{μ} includes emergent gauge fields:

$$D_{\mu} = \partial_{\mu} - ig A_{\mu}^{a}(x) T^{a} - ig' Y B_{\mu}(x).$$

The scalar field $\Phi(x)$ enforces projection filtering through the operator Π_{Φ}, aligning internal vector orientations. When Φ acquires a nonzero vacuum expectation value (VEV), $\langle \Phi(x) \rangle = v/\sqrt{2}$, this projection becomes fixed, and the internal structure of $\chi(x)$ becomes locked to the scalar manifold.

A.2   Projection-Induced Mass Terms

We begin with the scalar-filtered kinetic term for the internal spinor:

$$\mathcal{L}_{\text{int}} = \chi^{\dagger}(x) \left(-D^{\mu} D_{\mu} \right) \chi(x),$$

where $\chi(x)$ transforms under internal $SU(2)_L \times U(1)_Y$ and is subject to projection filtering via Π_{Φ}. This term arises directly from the master Lagrangian (see Appendix M of *The Axis Model*) and reflects the quantized dynamics of internal vector displacements within the scalar-coherent subspace. Prior to scalar alignment, Π_{Φ} dynamically filters internal field configurations, suppressing incoherent excitations and enforcing gauge covariance, consistent with the BRST-consistent structure of the model (cf. Section 2.2 of *Quantum Completion*).

When the scalar field acquires a vacuum expectation value, $\langle \Phi(x) \rangle = v/\sqrt{2}$, the projection operator Π_{Φ} becomes fixed, selecting a unique coherence frame for all internal excitations. This fixed background explicitly breaks internal rotational symmetry in the spinor kinetic term. The projection-aligned manifold defines a geometric medium through which fluctuations in the gauge fields incur an energetic cost.

---

[10]While $\chi(x)$ defines the internal projection space that sources the $SU(2)$ gauge curvature, the W and Z bosons are not constrained to decay solely into particles sharing the same compositional basis. Instead, they couple to all morton-structured fermions with appropriate $SU(2)$ and $U(1)$ quantum numbers, as defined in the internal configuration geometry. Thus, standard electroweak decay channels remain fully preserved.

To see how mass terms arise, we expand the covariant derivative to second order in gauge field fluctuations. The operator $-D^\mu D_\mu$ includes both first- and second-order gauge field couplings. The second-order terms yield:

$$\chi^\dagger \left[g^2 A_a^\mu A_{a\mu} T^a T^a + g'^2 Y^2 B^\mu B_\mu + 2gg' A_3^\mu B_\mu T^3 Y \right] \chi.$$

These quadratic terms are not artifacts of gauge redundancy. Once scalar coherence locks the projection geometry, the internal space is no longer gauge-deformable. Gauge field propagation introduces a *projection mismatch*—an energetic incompatibility between the fluctuating field directions and the fixed internal alignment induced by Φ.

The residual curvature from this mismatch persists in the filtered energy functional and acquires a scalar-normalized prefactor:

$$\mathcal{L}_{\text{mass}} = \frac{v^2}{8} \left[g^2 (A_\mu^1)^2 + g^2 (A_\mu^2)^2 + (g A_\mu^3 - g' B_\mu)^2 \right], \tag{78}$$

which exactly reproduces the electroweak boson mass matrix structure. In the Axis Model, this mass does not arise from spontaneous symmetry breaking of a fundamental Higgs doublet, but from the *energetic cost of a projection mismatch* between scalar-locked coherence and gauge field fluctuations.

A.3 Physical Interpretation

The scalar field $\Phi(x)$ acts as a coherence modulator that filters internal field configurations. Once Φ develops a VEV, it locks internal vector orientations, modifying the spectrum of allowable internal transitions. This locking introduces curvature in the gauge sector: the kinetic energy of $\chi(x)$—when filtered through the fixed Π_Φ—contains residual curvature contributions that manifest as mass terms for gauge bosons.

This mechanism is consistent with the geometric logic of the Axis Model: - Gauge bosons emerge from internal vector symmetry projections, - Masses arise only when scalar coherence symmetry is spontaneously broken, - The vacuum expectation value of Φ defines the scalar coherence scale v, - No scalar doublet is needed, and no ad hoc Yukawa couplings are introduced.

A.4 Distinction from the Standard Model

In the Standard Model, masses arise from the kinetic term $|D_\mu \Phi_H|^2$ where Φ_H is a complex scalar SU(2) doublet. In the Axis Model, the scalar Φ is a singlet under SU(2) but dynamically governs the projection alignment of internal doublet configurations. The gauge boson mass terms arise from scalar-curvature backreaction on internal spinor dynamics, not from coupling to a fundamental Higgs field.

Thus, while the final mathematical structure of the mass terms matches the Standard Model, the physical origin is distinct.

B Projector Kernels, θ–Z_μ Diagonalization, and the Leading–Log Gaussian Filter

Throughout we expand the scalar about its coherent background, $\Phi = v + \varphi$, and denote the massive internal vector(s) by $V_\mu \in \{X_\mu, Z_\mu\}$ with $m_V^2 = g_{\Phi V}^2 v^2$. Yukawa coupling to a Dirac fermion is $y \equiv g_{\psi\Phi}$, and the derivative mixing is $g_Z (\partial_\mu \Phi) Z^\mu$ as in the master Lagrangian. We work in dimensional regularization, $d = 4 - 2\epsilon$, and the $\overline{\text{MS}}$ scheme. Passarino–Veltman functions are $A_0(m^2)$ and $B_0(p^2; m_1, m_2)$ with $\Delta \equiv \frac{1}{\epsilon} - \gamma_E + \ln 4\pi$.

B.1 (A) 1PI kernels for γ_Π at $O(g_{\Phi V}^2)$ and $O(y^2)$; bubble–chain resummation

Operator viewpoint. Model the projector as a composite operator acting on the Abelian-basis tensor in the projected connection:

$$V_\mu \;=\; \Pi_\Phi[\Phi, \partial\Phi; \mu] \cdot \mathcal{V}_\mu[X, Z, q], \qquad A_\mu^a = \text{Tr}\,[T^a V_\mu]. \tag{79}$$

To leading derivatives we parameterize

$$\Pi_\Phi = 1 - c_1(\mu)\frac{\partial^2}{\Lambda_\Pi^2} - c_2(\mu)\frac{(\partial\theta)^2}{\Lambda_\Pi^2} + \cdots, \qquad \Phi = |\Phi|e^{i\theta}. \tag{80}$$

The anomalous dimension $\gamma_\Pi(\mu) \equiv -\mu\frac{d}{d\mu}\ln Z_\Pi$ is determined by the renormalization of the coefficients $c_{1,2}$ via the 1PI two-point kernels that dress the derivative structures.

Feynman rules (around v). From $\frac{1}{2}g_{\Phi V}\Phi^2 V_\mu V^\mu$:

$$\varphi V_\mu V_\nu : \quad i\, 2g_{\Phi V} v\, \eta_{\mu\nu}, \tag{81}$$

$$\varphi\varphi V_\mu V_\nu : \quad i\, g_{\Phi V}\, \eta_{\mu\nu}. \tag{82}$$

From the Yukawa $y\,\varphi\,\bar\psi\psi$: $\varphi\,\bar\psi\,\psi : i\,y$. Vector propagator (massive, R_ξ):

$$\Delta_V^{\mu\nu}(p) = \frac{-i}{p^2 - m_V^2}\left(\eta^{\mu\nu} - \frac{p^\mu p^\nu}{p^2}\right) - i\,\xi\,\frac{p^\mu p^\nu}{(p^2 - \xi m_V^2)\,m_V^2}. \tag{83}$$

Fermion propagator: $S_\psi(p) = \frac{i(\not{p}+m_\psi)}{p^2 - m_\psi^2}$.

Scalar self-energy from vector loops, $\Sigma_\varphi^{(V)}(p^2)$. The 1PI scalar two-point function at $O(g_{\Phi V}^2)$ is given by the bubble with two φVV vertices:

$$i\Sigma_\varphi^{(V)}(p^2) = (i\,2g_{\Phi V}v)^2 \int \frac{d^d k}{(2\pi)^d}\,\Delta_V^{\mu\nu}(k)\,\Delta_V^{\rho\sigma}(k+p)\,\eta_{\mu\rho}\eta_{\nu\sigma}. \tag{84}$$

In terms of PV functions one may write

$$\Sigma_\varphi^{(V)}(p^2) = \frac{(2g_{\Phi V}v)^2}{16\pi^2}\Big[(d-1)\,B_0(p^2; m_V, m_V) + \mathcal{F}_\xi(p^2; m_V)\Big], \tag{85}$$

where $\mathcal{F}_\xi$ encodes gauge-parameter-dependent longitudinal pieces (cancelling in physical projections). The wavefunction renormalization is

$$\delta Z_\varphi^{(V)} = -\left.\frac{d\Sigma_\varphi^{(V)}}{dp^2}\right|_{p^2=\mu^2} = -\frac{(2g_{\Phi V}v)^2}{16\pi^2}\Big[(d-1)\,B_0'(\mu^2; m_V, m_V) + \cdots\Big]. \tag{86}$$

For $|\mu^2| \ll m_V^2$, $B_0'(0; m, m) = 1/(6m^2)$, giving the expected *positive* finite wavefunction dressings; the ξ-dependence is subleading and cancels in gauge-invariant observables built from the projected connection.

Scalar self-energy from fermion loops, $\Sigma_\varphi^{(\psi)}(p^2)$.

$$i\Sigma_\varphi^{(\psi)}(p^2) = (-1)\,(iy)^2 \int \frac{d^dk}{(2\pi)^d}\, \mathrm{tr}[S_\psi(k)\,S_\psi(k+p)]$$

$$= \frac{y^2}{4\pi^2}\Big\{ A_0(m_\psi^2) - \frac{1}{2}\big[(4m_\psi^2 - p^2)B_0(p^2; m_\psi, m_\psi) - 2A_0(m_\psi^2)\big]\Big\}. \tag{87}$$

Thus

$$\delta Z_\varphi^{(\psi)} = -\left.\frac{d\Sigma_\varphi^{(\psi)}}{dp^2}\right|_{p^2=\mu^2} = -\frac{y^2}{16\pi^2}\Big[\tfrac{1}{3} + \ln\frac{\mu^2}{m_\psi^2} + \cdots\Big], \tag{88}$$

where the ellipsis encodes finite scheme-dependent constants and mass ratios.

From δZ_φ to γ_Π. The derivative operators inside Π_Φ renormalize with the same counterterms that renormalize φ's kinetic term at leading derivatives. Denoting by C_V and C_y the scheme- and gauge-independent combinations extracted from the UV poles of the two kernels,

$$\gamma_\Pi(\mu) = \frac{1}{16\pi^2}\Big(C_V\, g_{\Phi V}^2(\mu) + C_y\, y^2(\mu)\Big) + \cdots, \qquad C_{V,y} > 0. \tag{89}$$

Bubble–chain resummation and the projector form factor. Let $c_1(\mu)$ multiply the leading ∂^2/Λ_Π^2 term of Π_Φ at scale μ. The RG equation reads

$$\mu\frac{dc_1}{d\mu} = \gamma_\Pi(\mu)\,c_1(\mu) \quad\Rightarrow\quad c_1(\mu) = c_1(\mu_0)\,\exp\Big[\int_{\mu_0}^\mu \frac{d\mu'}{\mu'}\,\gamma_\Pi(\mu')\Big]. \tag{90}$$

Repeated (leading-log) insertions of the ∂^2 kernel in the projector line build the bubble chain. At external momentum p this resums to the multiplicative *form factor*

$$\mathcal{F}_\Pi(p^2; \mu) = \exp\Big[-\,\Xi(\mu)\,\frac{p^2}{\Lambda_\Pi^2} + \cdots\Big], \qquad \Xi(\mu) \equiv \int_{\mu_0}^\mu \frac{d\mu'}{\mu'}\,\gamma_\Pi(\mu'). \tag{91}$$

The projector loses a controlled derivative expansion when $\Xi(\Lambda_\Phi) \simeq 1$.

B.2 (B) θ–Z_μ quadratic kernel and field-space diagonalization

Quadratic action. For $\Phi = |\Phi|e^{i\theta}$ and expanding about v, the phase sector and the derivative mixing give (momentum space)

$$S_{\theta Z} = \frac{1}{2}\int \frac{d^4p}{(2\pi)^4}\, \begin{pmatrix} \theta(-p) & Z_\mu(-p) \end{pmatrix} \begin{pmatrix} K_\theta(\mu)\,p^2 & ig_Z\,p_\nu \\ -ig_Z\,p_\mu & -\mathcal{K}_Z^{\mu\nu}(p) \end{pmatrix} \begin{pmatrix} \theta(p) \\ Z_\nu(p) \end{pmatrix}, \tag{92}$$

with the R_ξ inverse propagator $\mathcal{K}_Z^{\mu\nu}(p) = (p^2 - m_Z^2)\,\eta^{\mu\nu} - (1 - \frac{1}{\xi})\,p^\mu p^\nu$, $m_Z^2 = g_{\Phi V}^2 v^2$, and $K_\theta(\mu) > 0$ the renormalized phase stiffness.

Field redefinition / Schur complement. Integrating out Z_μ (or completing the square) yields the effective θ kernel

$$K_\theta^{\mathrm{eff}}(p^2; \mu) = K_\theta(\mu)\,p^2 - g_Z^2\,p_\mu\,\Delta_Z^{\mu\nu}(p)\,p_\nu, \tag{93}$$

$$\Delta_Z^{\mu\nu}(p) = \frac{-i}{p^2 - m_Z^2}\Big(\eta^{\mu\nu} - \frac{p^\mu p^\nu}{p^2}\Big) - i\xi\,\frac{p^\mu p^\nu}{(p^2 - \xi m_Z^2)\,m_Z^2}. \tag{94}$$

Contracting with $p_\mu p_\nu$ selects only the longitudinal part: $p_\mu \Delta_Z^{\mu\nu} p_\nu = -i\, \frac{\xi p^2}{p^2 - \xi m_Z^2}$. Hence

$$K_\theta^{\text{eff}}(p^2; \mu) = K_\theta(\mu)\, p^2 \left[1 - \frac{\xi\, g_Z^2}{K_\theta(\mu)}\, \frac{p^2}{m_Z^2}\, \frac{1}{1 - \frac{p^2}{\xi m_Z^2}} \right]^{-1}, \tag{95}$$

which, for $|p^2| \ll m_Z^2$, reduces to

$$K_\theta^{\text{eff}}(p^2; \mu) = K_\theta(\mu)\, p^2 \left[1 - \frac{\xi\, g_Z^2}{K_\theta(\mu)}\, \frac{p^2}{m_Z^2} + O\!\left(\frac{p^4}{m_Z^4} \right) \right]^{-1}. \tag{96}$$

The bracket is the origin of the main-text $(1 - \alpha\, p^2/m_Z^2)^{-1}$ factor; gauge-parameter dependence is absorbed into K_θ at this order, and physical conclusions are unchanged.

B.3 (C) Leading–log equivalence and the emergent Gaussian filter

Common derivative dressings. The projector route (Appendix B.1) and the phase-kernel route (Appendix B.2) are governed by the same family of diagrams: vector and fermion loops that dress *derivative* structures of the scalar sector. Let $c_1(\mu)$ multiply $(\partial\theta)^2/\Lambda_\Phi^2$ in the long-wavelength phase action; to leading logs,

$$\mu \frac{dc_1}{d\mu} = \gamma_\Pi(\mu)\, c_1(\mu), \qquad \gamma_\Pi(\mu) = \frac{1}{16\pi^2}\left(C_V\, g_{\Phi V}^2 + C_y\, y^2 \right) + \cdots, \tag{97}$$

with the *same* coefficients C_V, C_y extracted from the UV poles of $\Sigma_\varphi^{(V)}$ and $\Sigma_\varphi^{(\psi)}$.[11] Solving gives $c_1(\mu) = c_1(\mu_0) \exp\!\left[\int_{\mu_0}^\mu \frac{d\mu'}{\mu'} \gamma_\Pi(\mu') \right]$, and inserting the resummed $c_1(\mu)$ into either the projector or the phase kernel produces the same momentum-space suppression of off-diagonal (non-Abelian) projections:

$$\boxed{\mathcal{F}_\Pi(p^2; \mu) = \exp\!\left[-\,\Xi(\mu)\, \frac{p^2}{\Lambda_\Pi^2} \right] \simeq \exp\!\left[-\,\frac{\langle(\partial\theta)^2\rangle_\mu}{\Lambda_\Phi^2} \right], \qquad \Xi(\mu) = \int_{\mu_0}^\mu \frac{d\mu'}{\mu'}\, \gamma_\Pi(\mu').} \tag{98}$$

The EFT ceases to have a controlled non-Abelian projection when $\Xi(\Lambda_\Phi) \simeq 1$, equivalently when $\langle(\partial\theta)^2\rangle_{\Lambda_\Phi} \simeq \Lambda_\Phi^2$ in the phase sector.

Remarks. (i) Gauge-parameter dependence drops out of leading logs that determine γ_Π and therefore $\Xi(\mu)$; scheme dependence only affects subleading finite terms. (ii) The Abelian basis remains perturbative at $\mu \simeq \Lambda_\Phi$; what fails is the projected *non-Abelian* identification. (iii) Matching to the gravitational extension's coherence filter $f(\Phi) = \exp\!\left[-|\nabla\theta|^2/\Lambda_\Phi^2 \right]$ follows by identifying $\langle(\partial\theta)^2\rangle_\mu$ with the renormalized gradient variance.

---

[11] This identification follows by matching counterterms in the derivative operator basis: $\delta\mathcal{L} \supset -\frac{1}{2}(\delta Z_\varphi)\,(\partial\varphi)^2 \leftrightarrow -c_1\,(\partial\theta)^2/\Lambda_\Phi^2$ at fixed v and to leading order in derivatives.